12-2009

EXPERIMENTAL CHARACTERIZATION OF STRESS RELAXATION IN GLASS

Hemanth Kadali
Clemson University, hkadali@clemson.edu

EXPERIMENTAL CHARACTERIZATION OF STRESS RELAXATION IN GLASS

A Thesis
Presented to
the Graduate School of
Clemson University

In Partial Fulfillment
of the Requirements for the Degree
Master of Science
Mechanical Engineering

---

by
Hemanth C Kadali
December 2009

Accepted by:
Dr. Vincent Blouin, Committee Chair
Dr. Paul Joseph
Dr. Richard Miller
Dr. Kathleen Richardson
Dr. Lonny Thompson

ABSTRACT

Glass viscoelasticity has gained importance in recent years as glass lens molding appeared as a valuable alternative to the traditional grinding and polishing process for manufacturing glass lenses. In the precision lens molding process, knowledge of viscoelastic properties of glass in the transition region, which affect the stress relaxation behavior, is required to precisely predict the final size and shape of molded lenses. The purpose of this study is to establish a step-by-step procedure for characterizing the viscoelastic behavior of glass in the glass transition region using a finite term Prony series of a Generalized Maxwell model. This study focuses on viscoelastic characterization of stabilized glass samples at lower stress levels between 3 and 12 MPa where it demonstrates *linearity*. Analysis and post-processing of creep data, performed in MATLAB and MAPLE, include displacement-to-strain conversion, determination of viscoelastic moments and constants, normalization, curve fitting and retardation-to-relaxation conversion. The process of curve fitting is carried out using a constrained optimization scheme to satisfy the constraint equations involving viscoelastic constants and functions. A set of relaxation parameters needed in numerical modeling, i.e., weights and times of the Prony series are presented in this thesis for borosilicate glass at different temperatures. Additionally, the issues related to the characterization of optical glasses were identified and discussed.

DEDICATION

To my parents Mr. Rao .V. Kadali and Mrs. Padmavathi Kadali

ACKNOWLEDGMENTS

I would like to thank my advisor, Dr. Blouin for his continuous support, encouragement and patience.

I would like to acknowledge all the Committee members, Dr. Kathleen Richardson, Dr. Paul Joseph, Dr. Lonny Thompson and Dr. Richard Miller, for providing their valuable input and for actively participating in decision making for recommendations of this study.

Additionally I would like to acknowledge Edmund Optics for its financial support, Dr. Rack for providing us access to his creep machines, Dr. Fotheringham for his guidance through glass workshop and Mr. David White for his help in setting up and troubleshooting the electronic equipment associated with the creep machine. I would like to acknowledge the glass blowers of the University of Georgia, Ricky Harrison and Brian Markowicz, for their dedication and interest in this project.

TABLE OF CONTENTS

Page

Table of Contents (Continued)

Page

Table of Contents (Continued)

Page

LIST OF TABLES

LIST OF FIGURES

List of Figures (Continued)

Figure Page

List of Figures (Continued)

Figure Page

CHAPTER 1

INTRODUCTION

1.1 Background

Glass viscoelasticity has gained importance in recent years as glass lens molding appeared as a valuable alternative to the traditional grinding and polishing process for manufacturing glass lenses. Viscoelasticity is a property of a material that exhibits both viscous and elastic behaviors. The viscoelastic properties of glass reveal themselves in the temperature range known as the transition region where, when stressed, the material displays an instantaneous strain as in case of an elastic body and a time-dependent strain as in case of a viscous body. Molding of the glass lens is carried out within the glass transition region where viscous properties are dominant [1]. In the precision lens molding process, knowledge of viscoelastic properties of glass in the transition region, which affect the stress relaxation, is one of the important behaviors required to precisely predict the final size and shape of molded lenses [2].

A full description of the viscoelastic behavior of glass encompasses the following aspects: (1) temperature-dependent viscosity, (2) shear and hydrostatic stress relaxation. This research focuses exclusively on the latter aspect.

Relaxation of viscoelastic materials can be obtained from one of the three following experiments: (1) measuring strain response at constant stress also known as creep experiments, (2) measuring stress response at constant strain also known as stress relaxation experiments, and (3) measuring the frequency-dependence of the viscoelastic modulus also known as dynamic methods. In this research, we make use of the first

method to investigate the viscoelastic behavior of borosilicate glass (commonly known as Pyrex®, a registered product of Corning Incorporated). The main motive behind the selection of creep experiments is the possibility to apply instantaneously and maintain a constant force on the sample using gravity since we do not have the capability to apply instantaneously a constant displacement required for stress relaxation.

Although we are interested in specific optical glasses such as LBAL35 and BK7, which are used in lens molding for their low glass transition temperature, we selected Pyrex® in this research for its ability to resist thermal shocks which makes it easy to manufacture samples of required shapes and sizes. The main limitation of this glass is that it is considered a *complicated* glass, which refers to the fact that it no longer follows a thermo-rheological simple (TRS) behavior during the phase transition [3, 4]. However, the method presented in this thesis can be applied to any type glass.

1.2 Research motivation

Ananthasayanam [5] developed a two-dimensional finite element numerical model to simulate the molding process and studied the effects of various parameters that affect the final size and shape of the lens after pressing. Parameters include friction between lens and molds, stress relaxation, structural relaxation, activation enthalpy and cooling rates. From his work he concludes that temperature-dependent stress relaxation parameters represent one of the most important aspects responsible for deviation of the lens profile. The motive behind this research is the lack of information on the viscoelastic parameters of specific glasses used in lens molding.

1.3 Research Goals

The main goal of this research is to characterize experimentally the stress relaxation behavior of glass in the transition region. This can be divided into the following research goals:

1. Study the manufacturability of specific glass samples into helical spring geometries for creep experiments,
2. Develop in-house capability based on the literature for conducting creep experiments on glass in the transition region, and
3. Develop a step-by-step procedure based on the literature for extracting numerically the stress relaxation parameters from experimental data.

1.4 An overview of the procedure

The stress relaxation behavior of glass can be fully described in different ways, such as using the KWW function [6] or a Prony series based on a generalized Maxwell model, which is the most widely accepted method and the focus of this research. In this method, relaxation parameters include shear and hydrostatic terms [7]. Pure shear data can be obtained directly from pure shear experiments. Knowing the shear behavior, the hydrostatic behavior can then be extracted from uni-axial experiments. Figure 1.1 shows a brief overview of all the important processes involved in characterization of stress relaxation of glass.

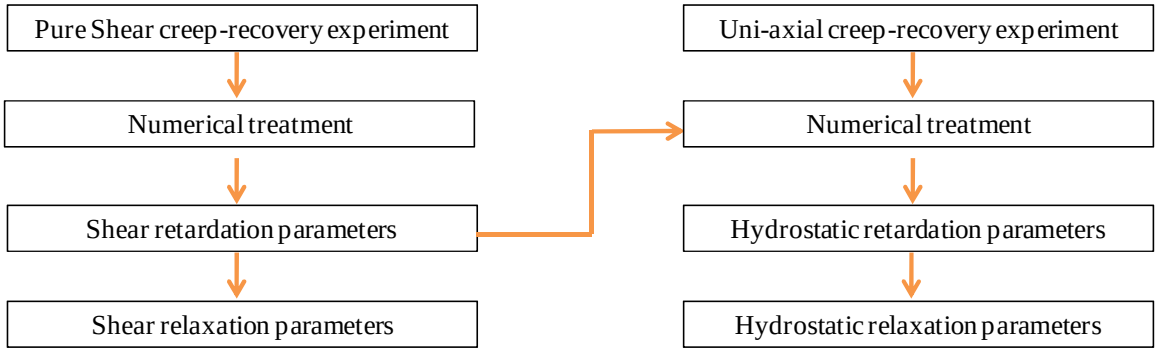

Figure 1.1. An overview of characterization process

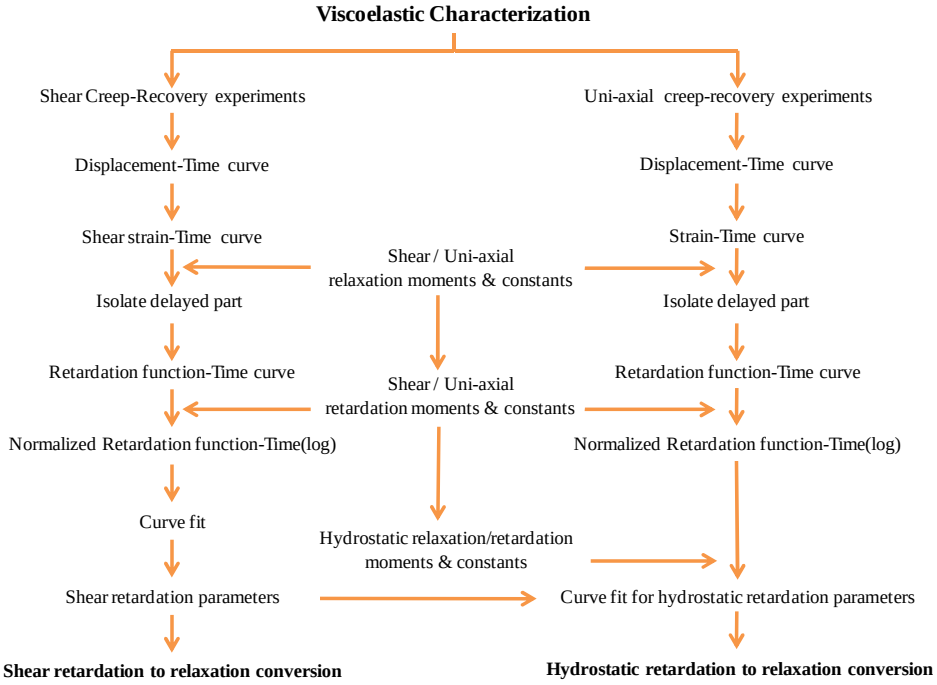

Figure 1.2. Anatomy of characterization process

Figure 1.2 illustrates a detailed version of Figure 1.1. A series of creep-recovery experiments were conducted at various temperatures and stress levels to study the viscoelastic behavior of glass. Shear creep-recovery experiments were carried out on helical glass spring samples to determine the shear retardation and relaxation viscoelastic

parameters. Shear retardation parameters are determined by curve fitting the experimental data with a Prony series of a generalized Maxwell's model while satisfying necessary constraints in terms of the calculated viscoelastic moments and constants. Shear retardation parameters are then converted to relaxation parameters through numerical treatment utilizing the viscoelastic constants and moments. A similar process is applied to the uni-axial creep experimental data up to the generation of the retardation function. Since the uni-axial retardation function is a combination of the known shear retardation function and the unknown hydrostatic function, the resultant uni-axial retardation experimental data is curve fitted to determine the unknown hydrostatic retardation parameters. Finally, the hydrostatic retardation parameters are converted into relaxation parameters.

The process of numerical treatment of raw creep data, i.e., conversions, isolation, shifting, normalizing and curve fitting, is automated using a MATLAB program (given in Appendices B and D). Retardation-to-relaxation conversions are automated using a MAPLE script (given in Appendices C and E).

1.5 Literature review

Several groups of researchers established the theory and experiments for viscoelastic characterization of glass during the last few decades. R.M. Christensen developed the concept of mathematical representation of stress relaxation behavior available in his book "Theory of Viscoelasticity". Rekhson [6] studied the relaxation behavior of various commercial glasses in the transition region on a device known as relaxo-meter specifically designed to carry out stress behavior measurements. Using this

device, he mathematically characterized the stress relaxation behavior of borosilicate glass in the transition region by the Kohlrausch-Williams-Watt (KWW) function given by:

$$\psi(t) = \exp\left[-\left(\frac{t}{\tau}\right)^{\beta}\right] \tag{1.1}$$

where ψ(t) is the time dependent relaxation function of time *t*, τ represents the relaxation time, and β is a constant. The apparatus utilizes the principle of dynamometer with a load cell to measure the stress decay with time. The operation of relaxo-meter resembles the present day lens molding process where the lower mold presses the glass perform against a fixed upper mold [8].

Previously the KWW function was utilized to fit the viscoelastic behavior of materials. Although the KWW function has limitations, it has been used for best describing mechanical and structural types of relaxation [9]. Both relaxation and retardation of glass can be fitted using this function also known as the "stretched exponential function". According to Rekhson [9], this function fails to correctly take relaxation mechanisms of glass into account on short-time scales as it gives an infinite relaxation rate at time zero. Duffrène *et al.* [7] explained further the inadequacies of the KWW function in characterizing the viscoelastic behavior of glass from creep-recovery experiments and proposed the generalized Maxwell model, represented by the Prony series shown in Eq. (1.2), as a more appropriate alternative,

$$\psi(t) = \sum_{j=1}^{n} w_{ij} \exp\left(-\frac{t}{\tau_{ij}}\right) \tag{1.2}$$

where w_{ij} and τ_{ij} are the relaxation weights and times, respectively and n is the number of terms of the Prony series. This function can be used to fit both relaxation and retardation functions precisely. The main advantage of the generalized Maxwell model over the KWW model is that it provides more flexibility for satisfying the theoretical constraints imposed by the viscoelastic functions and constants [7]. Gy *et al.* [10] developed the concept of viscoelastic constants which incorporates physical meaning into the glass characterization process. Viscoelastic constants were used to study the linear and thermo-rheological simple behavior of glass in the transition region as compared to variable β in the KWW function. The concept of viscoelastic constants and moments is explained in detail in Chapter 2.

In general glass demonstrates a linear viscoelastic behavior as long as stresses are low, namely 3 to 10 MPa [11] . By linearity we mean that the viscoelastic constants are independent of stress in the glass transition region within confined stress levels [7]. Duffrène *et al.* [7] characterized soda-lime-silica glass using both models for comparison purposes between 3 and 12 MPa and in a temperature range of 530˚C to 600˚C. They studied soda-lime-silica glass in the transition region by conducting a series of creep-recovery experiments of helical glass spring and rectangular glass rod specimens. According to Rekhson [11], linear behavior is also displayed by glasses with complicated thermal histories between stress levels of 3 to 10 MPa. In this thesis, the same concept is applied to a complicated glass (borosilicate glass) to characterize it in the linear region.

Viscosity of oxide glasses is measured from the Arrhenius equation explained in detail in Chapter 2. Duffrène *et al.* [7] measured the viscosity of soda-lime-silica glass

from the Arrhenius equation. Since borosilicate glass is considered complicated, it does not follow the Arrhenius equation for viscosity. Rekhson *et al.* [6] measured and reported the viscosity of borosilicate glass from an alternative method involving glass spring elongation at specific temperatures. Temperature dependent viscosity data for Pyrex® glass is available in the literature [6, 12].

Duffrène *et al.* [7] measured the mechanical properties (E, G, υ) of the soda-lime silica glass in the transition region using Brillouin's scattering experiment and assumed them to be constant over the temperature range. Temperature dependent mechanical properties of borosilicate glass are available in the literature published by Sam Spinner [13]. The elastic moduli of glasses at elevated temperatures were measured using dynamic resonance method. Temperature dependent mechanical properties of borosilicate glass were used in this research. Sensitivity analysis has been carried out in this thesis to investigate the validity of the assumption of mechanical properties being constant in the transition region.

1.6 Thesis outline

This dissertation is divided into eight chapters. Chapter 2 describes the conceptual background of viscoelasticity along with a focus on glass behavior in the transition region, mathematical interpretation of Maxwell's model, determination of mechanical properties and creep testing methods. Chapter 3 elucidates the process of glass manufacturing which includes helical spring and dog-bone samples and the issues arising during this process. In Chapter 4, the creep testing apparatus is described in detail. Chapter 5 presents the numerical treatment of the experimental data to extract the shear

stress relaxation properties. In Chapter 6, a sensitivity analysis of various process variables on relaxation parameters is presented. Chapter 7 consists of the procedure for extracting hydrostatic relaxation parameters from uni-axial and shears experiments. Chapter 8 concludes the thesis with a section on recommendations and future work.

CHAPTER 2

AN OVERVIEW ON VISCOELASTICITY IN GLASS

2.1 Glass terminology

This section includes several important terms used in the following sections.

Strain point: Temperature above which glass relieves stresses over time. It marks the low-temperature end of the glass transition region. If a glass sample is cooled below the strain point, any remaining stress would be locked, i.e., stress would not relax. The strain temperature is 510˚C for borosilicate glass [14].

Annealing point: Temperature above which stresses rapidly relax. Annealing is generally carried out at a viscosity of 10^{12} Pa·s.

Significance of annealing: Variations in cooling rates between the inside and outside regions of the glass induce thermal stresses. The inside region is comparatively at a higher temperature leading to expansion while the outside region contracts due to faster cooling. If the glass is cooled too fast, this expansion and contraction are locked into place leading to residual stresses. Thus, glass will eventually crack to relieve this built up stress. Annealing temperature for borosilicate glass is 565˚C [14].

Softening point: Temperature above which glass extends/deforms due to its own weight. Softening temperature for borosilicate glass is 820˚C [14].

Viscosity: Viscosity is a measure of the material's resistance to deformation. Usually viscosity varies with temperature following the Arrhenius law, given by

$$\frac{1}{\eta} = Ae^{-\frac{E}{RT}} \tag{2.1}$$

where A is a constant, E is the activation energy, R is the gas constant and T is the absolute temperature.

2.2 Glass transition temperature and its significance

Before understanding the meaning of glass transition, it is important to know about crystalline, amorphous and semi-crystalline solids. Crystalline solids have long range atomic order with respect to their position of atoms whereas amorphous solids have no long range atomic order of their position of atoms. However they can have local arrangement of atoms at atomic length scale due to the nature of chemical bonding. Semi-crystalline solids are a combination of both crystalline and amorphous parts. It is well known that glass is an amorphous solid. As shown in Figure 2.1, amorphous solids can be either in glassy or rubbery state based on the temperature. The temperature at which the transition from glassy state to rubbery state takes place in an amorphous solid is called the transition temperature [15]. Glass transition temperature is not a fixed parameter since glass phase in not in equilibrium. Important factors that affect the transition temperature value, T_g, are: (1) thermal history, i.e., rate of cooling and heating, (2) age, (3) molecular weight, and (4) method employed to measure T_g. Figure 2.1 shows the definition of the transition temperature as the point of intersection of the tangents to the glassy and rubbery curves. Note that the transition temperature is different from the melting temperature, which is a characteristic of crystals while transition temperature is a characteristic of amorphous solids [15].

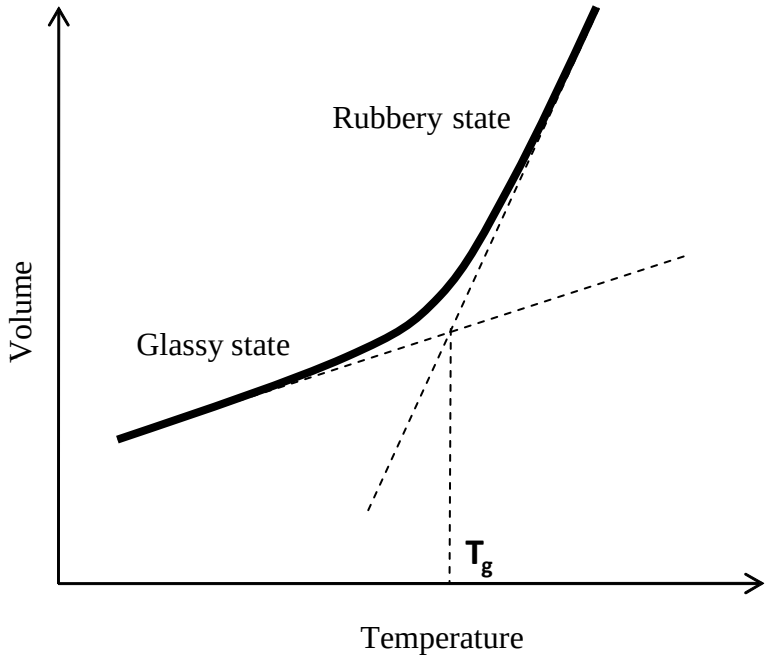

Figure 2.1. Glass transition region determined by Thermo Mechanical Analysis (TMA)

The glass transition temperature, T_g, for a given material is estimated using various methods such as Thermo Mechanical Analysis (TMA) and Differential Scanning Calorimetry (DSC) [15]. In the DSC method, the difference between the amount of heat required to increase the temperature of a given sample and a known reference are measured as a function of temperature.

2.3 Viscoelasticity

Viscoelasticity is a property of the material that exhibit both elastic and viscous behavior while undergoing deformation. These materials can be graphically and mathematically modeled by combining elements that represent these characteristics i.e. they can be represented as a combination of springs and dashpots as shown in Figure 2.2.

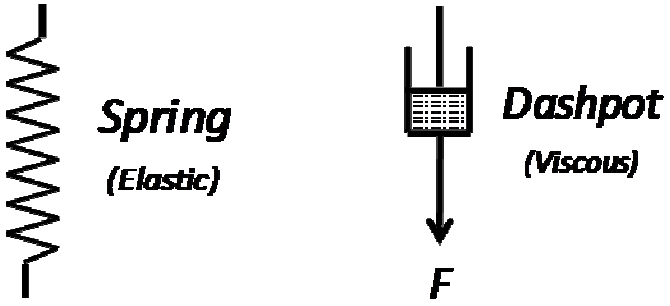

(a) (b)

Figure 2.2. Elements of Maxwell model: (a) Spring (b) dashpot (piston and cylinder assembly)

Mathematically, a spring demonstrates Hookean behavior for solids and a dashpot demonstrates Newtonian law for liquids. According to Hooke's law of solids,

$$\varepsilon = \frac{\sigma}{E} \tag{2.3}$$

where ε is the strain, σ is the stress and E is Young's modulus of elasticity of the material at room temperature.

The delayed version of the viscoelastic material demonstrates non-Hookean behavior and resembles Newtonian materials where stress is proportional to the first derivative of strain [16].

Newtonian law of liquids is given by

$$\frac{d\gamma}{dt} = \frac{\sigma}{\eta} \tag{2.4}$$

where γ is the strain, σ is the stress and η is the viscosity of the fluid inside the dashpot. According to Newtonian law of liquids there is a linear dependence of rate of shear strain to applied stress.

2.4 Stress relaxation and creep

The property of viscoelasticity induces non-linearity into the behavior of material. This non-linearity can be defined by both stress relaxation and creep. Stress relaxation can be defined as time dependent decrease in stress under a constant strain or deformation in the viscoelastic region. It other words, it is the stress decay during creep in transition region. Contrary to stress relaxation, creep refers to the study of strain behavior on application of constant stress. Creep-recovery experiments are comparatively easier than perform stress relaxation experiments. Creep recovery experiments are considered advantageous over stress relaxation experiments due to the fact that it is possible to extract high sensitive creep-recovery data when compared to low sensitive stress decay measurement from stress relaxation tests. Stress relaxation and creep are complimentary.

2.4.1 Strain behavior of glass at constant stress in various temperature zones

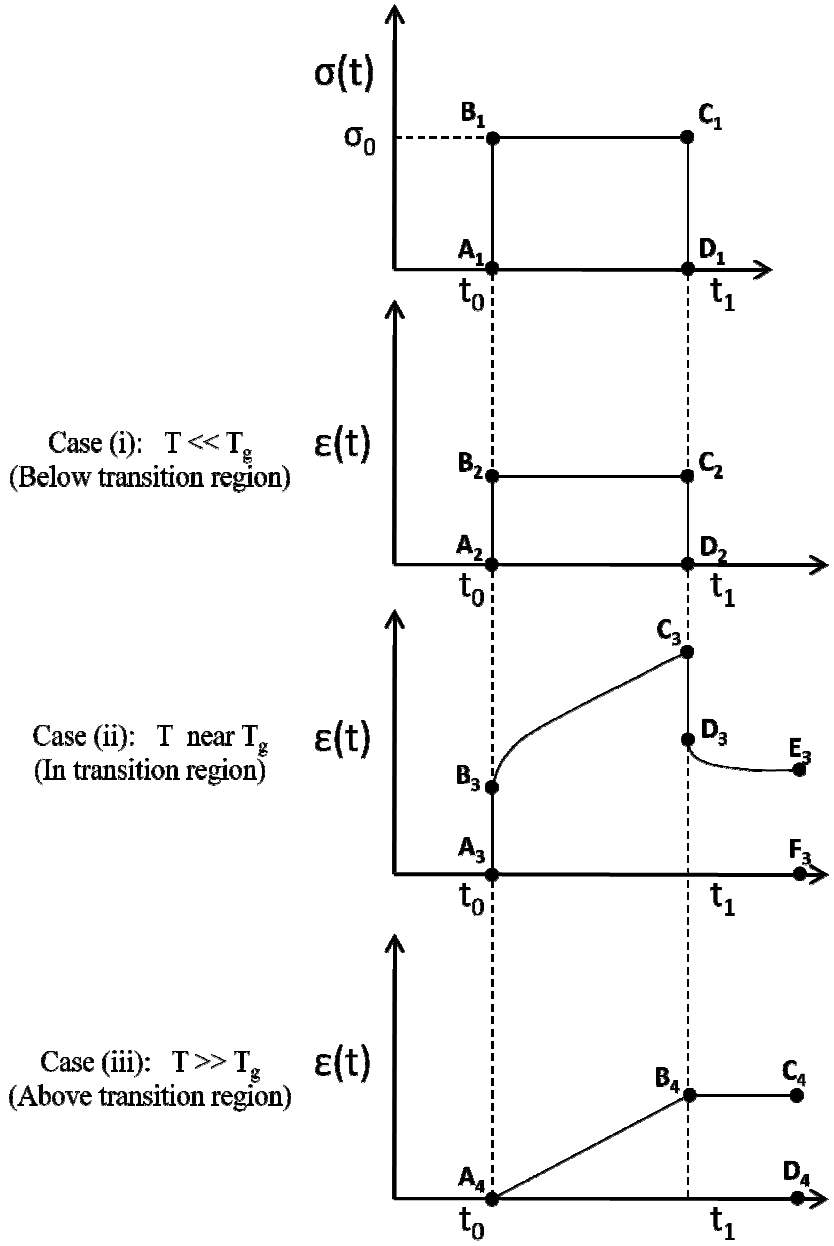

Figure 2.3. Strain behavior of glass at constant stress in various temperature zones

A constant stress σ_0 is applied on a glass rod at time t_0 and removed at time t_1. Following behavior of glass can be observed based on the region of temperature the glass is loaded: From Figure 2.3

Case (i): Below Transition region: Segment A_2-B_2-C_2-D_2 is the behavior of glass on application of constant stress σ_0 (segment A_1-B_1-C_1-D_1). In this region glass acts as an elastic body. Strain (segment A_2-B_2) due to application of constant stress σ_0 is fully recovered (segment C_2-D_2) on its removal. Conceptually, segment A_2-B_2 is equal to segment C_2-D_2.

Case (ii): In the Transition region: Segment A_3-B_3-C_3-D_3-E_3 is the behavior of glass on application of constant stress σ_0 (segment A_1-B_1-C_1-D_1). In this region glass displays both viscous and elastic properties. There is an instantaneous strain (segment A_3-B_3) produced as in case(i) due to application of constant stress σ_0 and time dependent strain (segment B_3-C_3) as in case(3) due to viscous part. When stress is removed there is an instantaneous recovery (segment C_3-D_3) which is equal to Segment A_3-B_3 as in case (i) and a time dependent recovery as in case (iii). This behavior is also termed as elastic recoiling. The length between points E_3 and F_3 is the non recoverable strain due to viscous part as in case (iii).

Case (iii): Above Transition region: Segment A_4-B_4-C_4 is the behavior of glass on application of constant stress σ_0 (segment A_1-B_1-C_1-D_1). Glass acts as a viscous material above transition region. There is no instantaneous strain due to application of constant stress σ_0. There is only the time dependent strain (segment A_4-B_4) due to the constant stress $\sigma_{0.}$ On removal of this stress, the strain does not recover as in case of elastic bodies. The length between points C_4 and D_4 is the non recoverable strain due to viscous part. It is the permanent viscous deformation.

2.4.2 Stress relaxation: stress response at constant strain

As defined earlier, when a body is subjected to a constant strain, there is a gradual decay in the stress known as stress relaxation. This is achieved through position control, i.e., the specimen is compressed or extended by a known distance resulting in a pre-determined strain as shown in Figure 2.4. Now the stress due to applied strain followed by the decayed stress is estimated from the load and position at the desired temperature in the glass transition region. Strain is maintained constant by keeping the displacement/position constant.

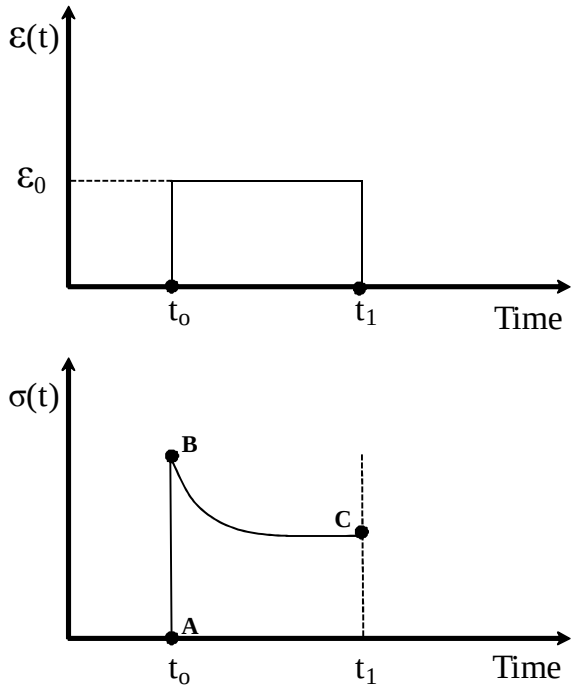

Figure 2.4 Stress relaxation at constant strain

2.4.3 Creep-recovery: strain response at constant stress

Behavior of the creep curve can be described by the following three important features as shown in Figure 2.5.

1) The instantaneous response, δ_i, is the instantaneous elongation of the glass sample due to instantaneous application of stress and the instantaneous recovery due to instantaneous unloading. δ_i is shown in Figure 4 as segments AB and CD, which are equal in magnitude.
2) The time-dependent loaded response (segment BC) is observed as long as the constant stress is applied.
3) The delayed recovery, δ_d, (segment DE) corresponds to the time-dependent recovery.

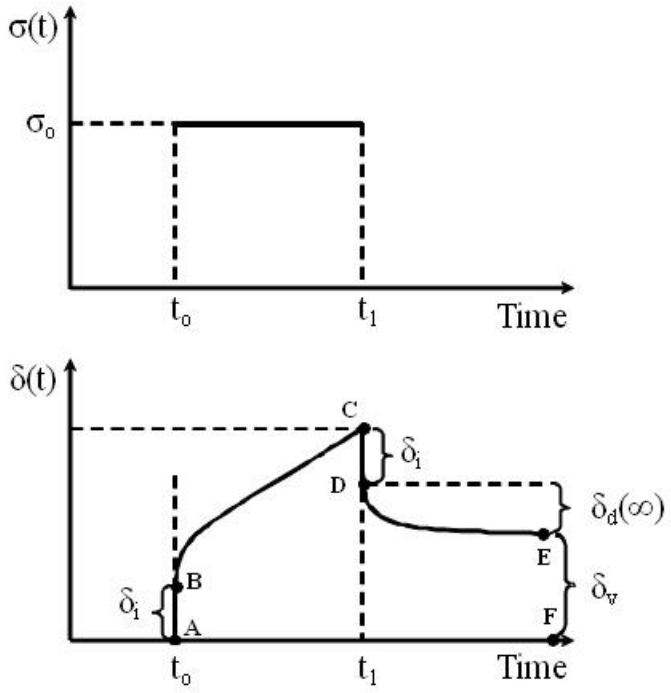

Figure 2.5 Strain behavior at constant stress

Uni-axial creep-recovery experiments on dog-bone samples constitute both shear and hydrostatic parts Therefore shear parameters are determined first from shear creep-

recovery experiments and hydrostatic parameters are then obtained indirectly from uni-axial and shear parameters through numerical treatment explained in Chapter 5.

2.5 Generalized Maxwell model

Viscoelastic behavior of glass can be theoretically expressed using a suitable series/parallel configuration of springs and dashpots. Instantaneous elongation is represented using springs, which are meant to describe Hookean elastic behavior, and dashpots, comprising of piston, cylinder and the viscous fluid describing Newtonian behavior as explained in section 2.1. Behavior of inorganic glasses cannot be fitted using a single Maxwell model or the Voight model. Therefore we need to venture into more complex models such as Burgers Model, KWW function and Maxwell's Model to characterize its behavior precisely [17]. Many models were proposed accordingly to fit the viscoelastic behavior of materials.

Maxwell's Model

Proposed by James Clerk Maxwell in 1867, is a model that combines a purely elastic spring and a purely viscous damper connected in series. As shown in Figure 2.6, the model is constrained at the top and an axial force F is applied on the other side.

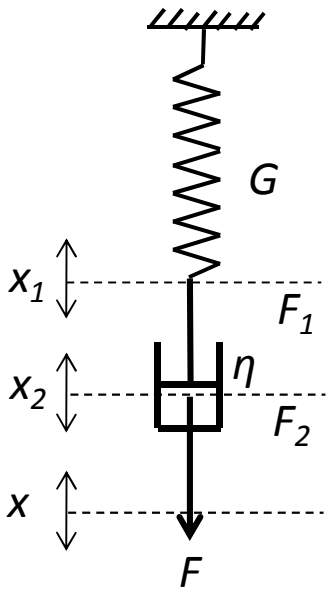

Figure 2.6 Maxwell model

In case of spring,

$$F_1 = k\ x \tag{2.5}$$

In case of dashpot,

$$F_2 = \eta\ \frac{A}{d}\ \frac{dy}{dt} \tag{2.6}$$

Maxwell model assumes a uniform distribution of stress over the individual elements. Mathematical interpretation [17] of this model is as follows:

(1) Total force acting on the model is equal to individual forces acting on the spring and the damper respectively and is expressed as

$$F = F_1 = F_2 \tag{2.7}$$

(2) Total stress acting on the model is equal to individual stresses acting on the spring and the damper respectively and can be expressed as

$$\sigma = \sigma_1 = \sigma_2 \tag{2.8}$$

(3) Total strain acting on the model is equal to individual strains acting on the spring and the damper respectively and can be expressed as

$$\varepsilon = \varepsilon_1 + \varepsilon_2 \tag{2.9}$$

(4) Total displacement of the model is equal to sum of individual displacements of spring and dashpot respectively and can be expressed as

$$x = x_1 + x_2 \tag{2.10}$$

(5) Relaxation is observed when total elongation is kept constant i.e. parameter x of Eqn (2.10) is a constant. Eqn. (2.11) is the derivative of Eqn. (2.10) with respect to time

$$\frac{dx_1}{dt} + \frac{dx_2}{dt} = 0 \tag{2.11}$$

(6) Time derivative of Eqn. (2.9) gives the strain rate. On substituting for F in the place of F_1 and F_2 results in the following important relation

$$x = \frac{F}{D} + \frac{F}{\eta \frac{A}{d}} t \tag{2.12}$$

(7) In order to maintain the elongation constant, the force F needs to be a function of time, which is given by

$$F(t) = kCe^{\frac{-t(kd)}{\eta A}} \tag{2.13}$$

(8) In Eqn. (2.13) $\frac{kd}{\eta A}$ is replaced with τ called Relaxation time

A simple Maxwell model is not sufficient to describe the behavior of glass since it cannot account for a retarded elastic response [17].

Generalized Maxwell's Model

As explained above, a single Maxwell model cannot fit the viscoelastic behavior of glass. Therefore a combination of Maxwell models arranged in parallel are considered to represent the viscoelastic behavior of glass mathematically.

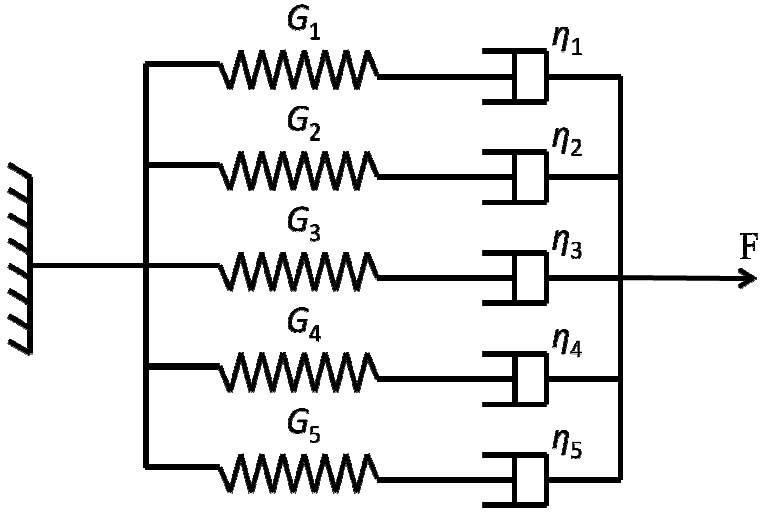

Figure 2.7. Generalized Maxwell model

The generalized Maxwell's model can be represented mathematically as shown below:

$$\Phi_i(t) = \sum_{j=1}^{m} \omega_{ij} \exp^{\frac{-t}{\tau_{ij}}} \tag{2.14}$$

where Φ(t) is the retardation function, i = 1,2,u based on whether the origin is shear (1), hydrostatic (2) or uni-axial (u), respectively. The number of terms, m, in the Prony series of a generalized Maxwell model is decided by the curve fitting process. Most commercial FEA solvers input glass viscoelastic behavior in terms of Prony series of a generalized Maxwell's model.

2.6 Stabilization of glass

Stabilization of glass refers to holding the glass sample at a given temperature until its properties no longer change with respect to time [17]. In the case of un-stabilized glass the viscosity changes with time. In this research creep-recovery experiments are conducted on stabilized glass samples. The glass samples are heated and soaked at the given temperature until properties stabilize. The soaking time varies with glass diameter.

2.7 Linearity and thermo-rheological simplicity

Linearity is the property of instantaneous and delayed elastic responses being linearly proportional to the applied stress [17]. Linearity is manifested in all glasses as long as the applied stresses are sufficiently low, i.e., creep curves are independent of applied stresses. This concept is also applicable to complicated glasses such as borosilicate glass. From a series of experiments conducted on different glasses, Rekhson concluded that the applied stresses should be in the range of 3-12 MPa for the glasses to describe linearity [11].

By Thermo-rheological simplicity we mean that the effect of temperature leads to a shift of the relaxation curve on the log scale without change in shape, i.e., the curves are parallel to each other as shown in Figure 2.8 and related using the Eqn.(2.15) [17].

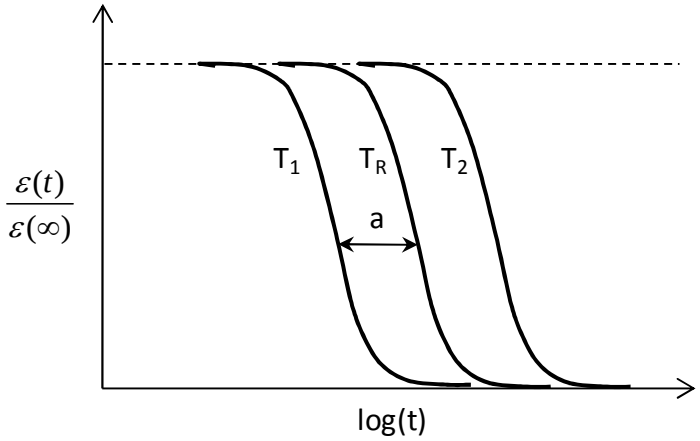

Figure 2.8. Thermo-rheological simple behavior

$$-\log a = A + \frac{B}{T} \tag{2.15}$$

where A and B are given by

$$A = -\log\left[\frac{\tau_r}{\tau_o}\right] \tag{2.16}$$

$$B = \frac{\Delta H}{R} \tag{2.17}$$

where, ΔH is is the activation energy, R is the gas constant and T is the absolute temperature .

If stress relaxation time follows the Arrhenius equation for viscosity, then viscosity is proportional to relaxation times and is given by.

$$\tau = \tau_0 \exp\left(\frac{\Delta H_i}{RT}\right) \tag{2.19}$$

In this case the curves demonstrate thermo-rheologically simple behavior. Borosilicate glasses are thermo-rheologically complex since their viscosity cannot be calculated from Arrhenius equation for viscosity [6].

2.8 Mechanical properties

Mechanical properties of glass generally change with temperature. Therefore there is a need for measuring temperature dependent mechanical properties in the transition region. In this research temperature dependent data of mechanical properties published in literature by Spinner [13] were used. The method that was employed by Spinner to measure temperature dependent mechanical properties is explained below.

Dynamic Resonance Method

Mechanical properties of materials can be measured at elevated temperatures using dynamic resonance method. In order to determine the mechanical properties at high temperatures it is important that the sample along with the setup is inside the furnace. As it is impossible to incorporate the setup inside the furnace, it is therefore extended into it through projections. These projections from the setup are in contact with the glass sample placed inside the furnace through small holes drilled through the thickness of the furnace. Glass specimen is vibrated using an oscillator at a particular frequency on one side and the other side consists of necessary arrangement for signal pickup. Knowing the dimensions of the sample, frequency of vibrations and mechanical properties of glass are calculated through numerical treatment [13].

2.9 Viscoelastic moments and constants

Tschoegl [18] introduced the term viscoelastic constants and moments and Duffrène and Gy [10] developed it as described below. Only specific concepts of interest are stressed in this section. Viscoelastic constants and moments are dimensionless quantities with some physical meaning. $<\tau_i^{\alpha}>$ and $<\lambda_i^{\alpha}>$ are the fundamental quantities representing relaxation and retardation moments and spectra respectively with i = 1,2 representing shear and hydrostatic, respectively, and α refers to the α^{th} order moment. In terms of continuous spectra they are defined by the following equations.

$$< \tau_i^{\alpha} >= \int_0^{+\infty} \tau^{\alpha} H_i(\tau) d\tau \tag{2.20}$$

$$\lambda_i^{\alpha} >= \int_0^{+\infty} \lambda^{\alpha} L_i(\lambda) d\lambda \tag{2.21}$$

where $H_i(\tau)$ and $L_i(\lambda)$ are relaxation and retardation spectra for subscript i = 1,2,u representing shear, hydrostatic and uni-axial, respectively.

Viscoelastic constants are the ratios of these viscoelastic moments and are explained in detail below.

1. Relaxation viscoelastic constant, Eqn. (2.22), is defined as the ratio of total delayed elasticity to instantaneous elasticity and is valid for i = 1,u, which represents shear and uni-axial, respectively.

$$\frac{< \tau_i^{\alpha} >}{< \tau_i >^{\alpha}} = \frac{\varepsilon_d(\infty) + \varepsilon_i}{\varepsilon_i} \tag{2.22}$$

2. Retardation viscoelastic constant characterizes the width of the retardation spectrum and is denoted as

$$\frac{<\lambda_i^{\alpha}>}{<\lambda_i>^{\alpha}}$$

The above ratio includes retardation moments which can be calculated using Eqn. (2.23)

$$<\lambda_i^{\alpha}>=\frac{1}{\Gamma(\alpha)}\int_0^{\infty} t^{(\alpha-1)}\Phi_i(t)dt \tag{2.23}$$

where Γ(α) is the gamma function.

3. Viscoelastic constant of creep-relaxation duality

$$\frac{<\lambda_i^{\alpha}>}{<\tau_i>^{\alpha}}$$

The individual components of this ratio, i.e., relaxation and retardation moments, can be calculated using Eqn. (2.23) and Eqn. (2.24).

$$\eta = G<\tau_1>=\frac{E<\tau_u>}{3} \tag{2.24}$$

Hydrostatic retardation/relaxation moments and constants are calculated from the shear and uni-axial moments and constants. The equations necessary for these inter-conversions are described in Chapter 7.

CHAPTER 3

GLASS GEOMETRY AND MANUFACTURING

3.1 Sample profiles

As discussed earlier in the previous sections, both shear and uni-axial creep-recovery data are required to characterize a given material. A few useful methods are described below. The main issue is to perform creep-recovery experiments on samples at elevated temperatures with all the required systems such as temperature measurement, displacement measurement, and gripping to be incorporated inside the furnace.

3.1.1 Pure shear experiments

Helical Spring

Creep-recovery experiments on spring samples yield pure shear data. The shear stress developed through the coil cross-section includes a large torsional shear component and a small transversal shear component. The calculations of stress are given in detail in Chapter 5. Springs can be tested in compression as well as tension, shown in Figure 3.1, both with advantages and limitations. The main issues relate to the ability to apply a perfectly centered load while maintaining the elongation of the sample in the axial direction. The main advantage of using helical spring sample over other types of specimens is its high sensitivity of deflection for a given stress [19].

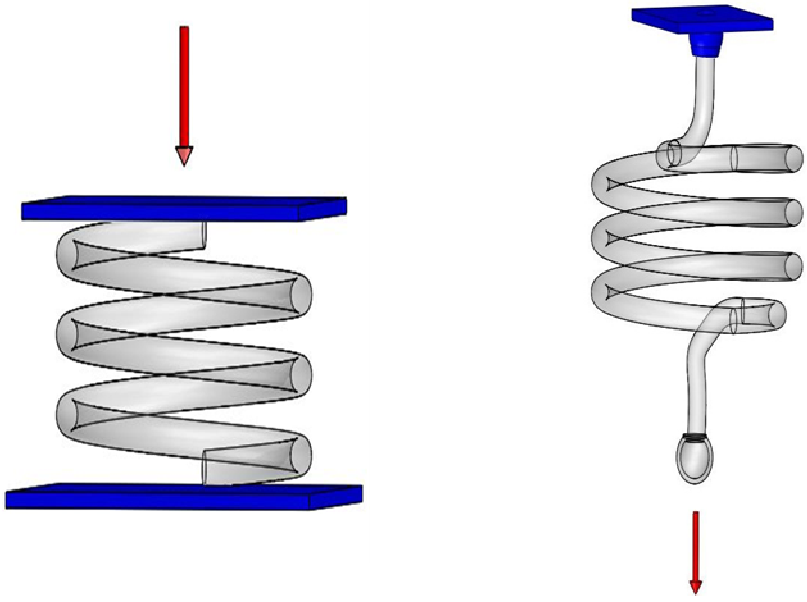

(a) (b)

Figure 3.1. Helical spring in (a) compression and (b) tension

Shaft in torsion

A circular shaft in torsion under a torque as shown in Figure 3.2 is another way of creating pure shear inside a sample. The resulting strain can be calculated from the angle of twist. The three main issues are:

(1) Constraining the shaft at one end,

(2) Applying a torque using gravity on the other end,

(3) Measuring the angle of twist using the LVDT.

(4) The entire system would have to be extended to inside of the furnace for measurements at elevated temperatures.

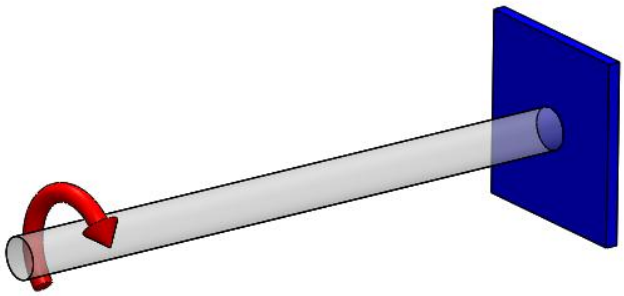

Figure 3.2. Glass rod subjected to torsion

3.1.2 Uni-axial experiments

Uni-axial creep-recovery experiments can be conducted on cylindrical or rectangular glass rods in compression or in tension to extract creep-recovery data. Compression of the sample is carried out between two parallel plates. One of the two sides is fixed and an axial force is exerted on the other side. The main difficulties that may arise are (1) the possibility of buckling if the sample is too long, and (2) the radial friction between the load application plate and the glass sample that might have a tendency to stiffen the system. During tension, a glass rod is constrained at one end and a downward axial force is applied on the other end. In both cases, strains are very small, therefore measuring the extension of the sample (of the order of several micro-meters) is generally very demanding. The total extension can be increased (1) by increasing the length of the sample up to the limit of temperature uniformity inside the furnace or (2) by increasing the load up to the limit of linear behavior of the glass.

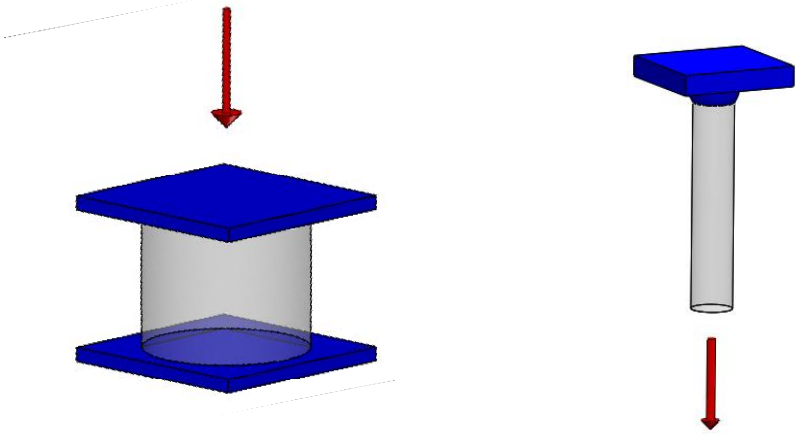

(a) **(b)**

Figure 3.3. Cylinderical glass rod in (a) compression (b) tension

3.2 Manufacturing helical spring samples

A helical spring, shown in Figure 3.4, is one of the few shapes that provide a pure shear behavior under longitudinal loading and is therefore ideal for shear-creep recovery experiments. However, manufacturing such springs is not an easy task. In this research, the helical spring samples, made of borosilicate glass, were manufactured manually by a professional glass blower. The samples were made from a long glass rod wrapped around a metallic shaft under the controlled heat of an oxy-acetylene torch. The samples were rigidly attached to the creep apparatus using metallic wires. The compliance of the end sections of the spring sample, i.e. above and below the coils including the grips, did not affect the results since the extensometer was attached to the coils. The coils were formed as closely as possible to each other to reduce the hydrostatic behavior and increase pure shear behavior.

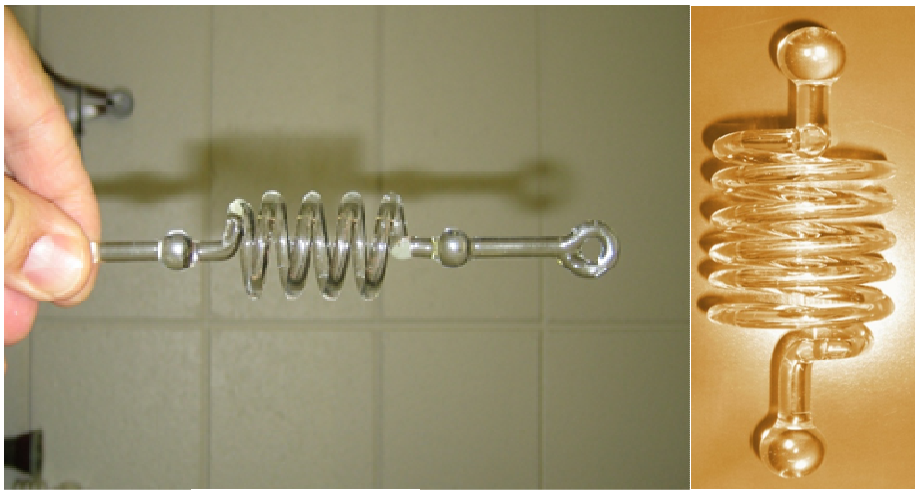

(a) (b)

Figure 3.4. Pyrex® spring samples

3.3 Optical glasses

As shown in Figure 3.5, several attempts were made to manufacture spring samples out of optical glass rods, generally known as low-Tg glasses for their low transition temperature. Examples of optical glasses include L-BAL35, N-FK5 and BK7. Compared to the behavior of Pyrex®, several interesting observations related to the manufacturing process of optical glasses include:

a. They are very sensitive to thermal shocks and rapid cooling. Long annealing processes are needed to avoid instantaneous fracture of the sample after manufacturing.
b. Reheating a damaged part of the sample results in immediate shattering if not carefully annealed. This makes it impossible to fix them once broken.
c. Optical glasses usually come as short rods (10 to 18 cm in length and 1 cm in diameter). Therefore, the rods must be extended before wrapping them into

springs. The extension process requires high temperature and large deformations of the glass, which may alter its optical, mechanical and thermal properties.

d. When melted and extended during the manufacturing process, many surface irregularities were observed.

e. They are prone to formation of bubbles when melted and extended.

f. Glasses with sand-blasted finish are much harder to work with than a smooth rod of the optical glass.

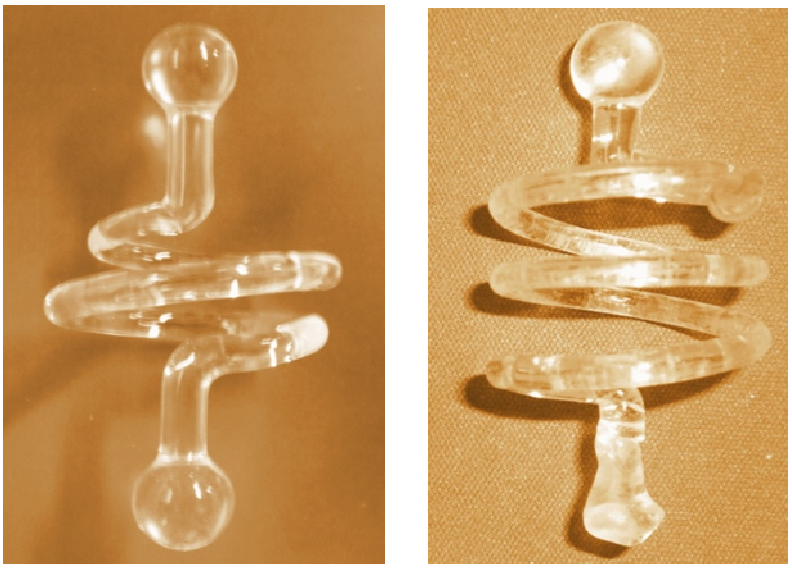

(a) (b)

Figure 3.5. (a) Spring made out of BK7 glass, (b) Spring made out of L-BAL35 glass

The glass blower should pay attention to the following points when forming spring glass samples.

a. Maximize uniformity of filament diameter as the glass is melted and extended. Having almost a uniform diameter throughout the glass sample depends mainly

on the expertise of the glass blower. If diameter is non-uniform, the non-uniformity can be incorporated in the numerical treatment of the experimental data by means of a specific shape factor using the average radius.

b. Careful annealing after forming is expected to prevent locking of stresses that could lead to fracture during the cooling process.

c. Minimize carbon residue coming from the torch during forming.

3.4 Manufacturing dog-bone samples

Manufacturing dog-bone samples from glass rods is quite simple compared to making spring glass samples. Assuming that glass rods of the required diameter are available, making dog-bone samples consists of cutting the rod to the proper length and forming the ends into balls using a torch. In this research, wing nuts were placed at both ends of the samples to facilitate the gripping process.

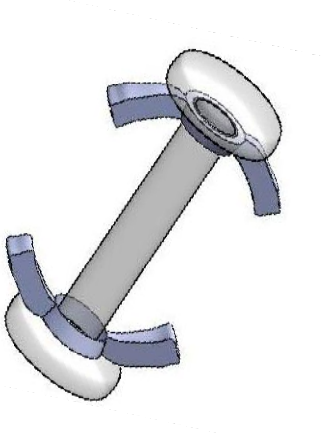

Figure 3.6. Dog-bone sample

CHAPTER 4

EXPERIMENTAL APPARATUS

4.1 Experimental setup

The experimental apparatus, shown in Figure 4.1, consists of a creep testing frame, vertical tube furnace, K-type thermocouples, temperature controllers, a loading/unloading mechanism, and a frictionless extensometer. The main features of this apparatus include: (1) the ability to apply and remove a constant instantaneous load on the sample using gravity, (2) maintain a constant and uniform temperature along the length of the sample, and (3) the ability to measure elongation without interfering with the sample's deformation.

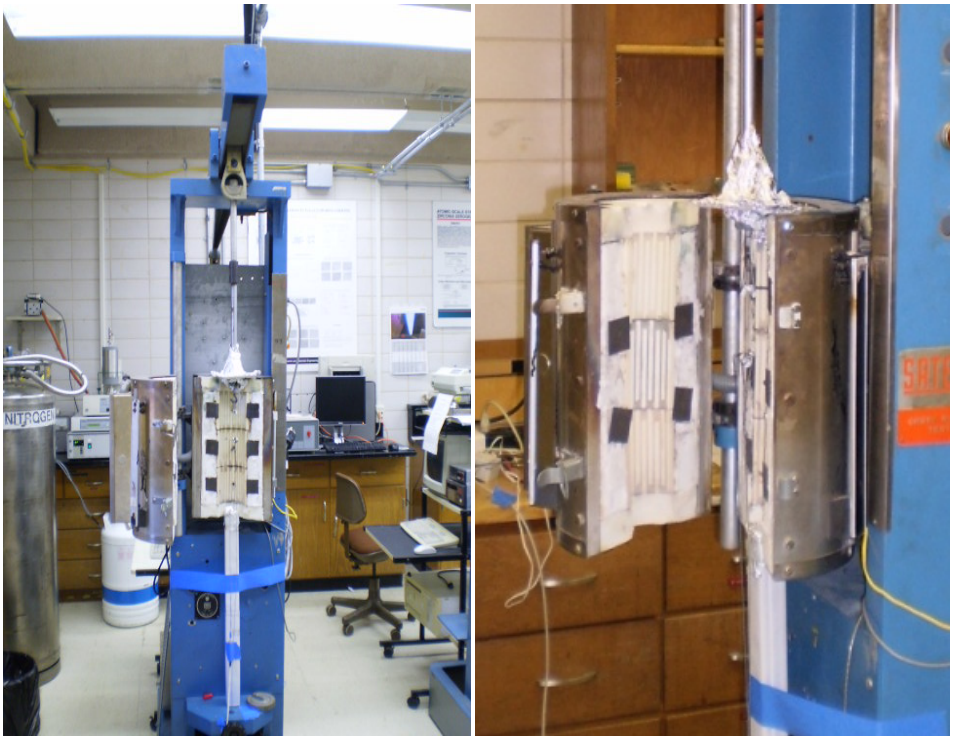

Figure 4.1 Creep apparatus

The glass sample is placed in the most uniform region of the furnace. As shown in Figure 4.2, rigid steel wires are used as extensions to connect the extensometer to two specific points of the glass sample to measure their relative displacement.

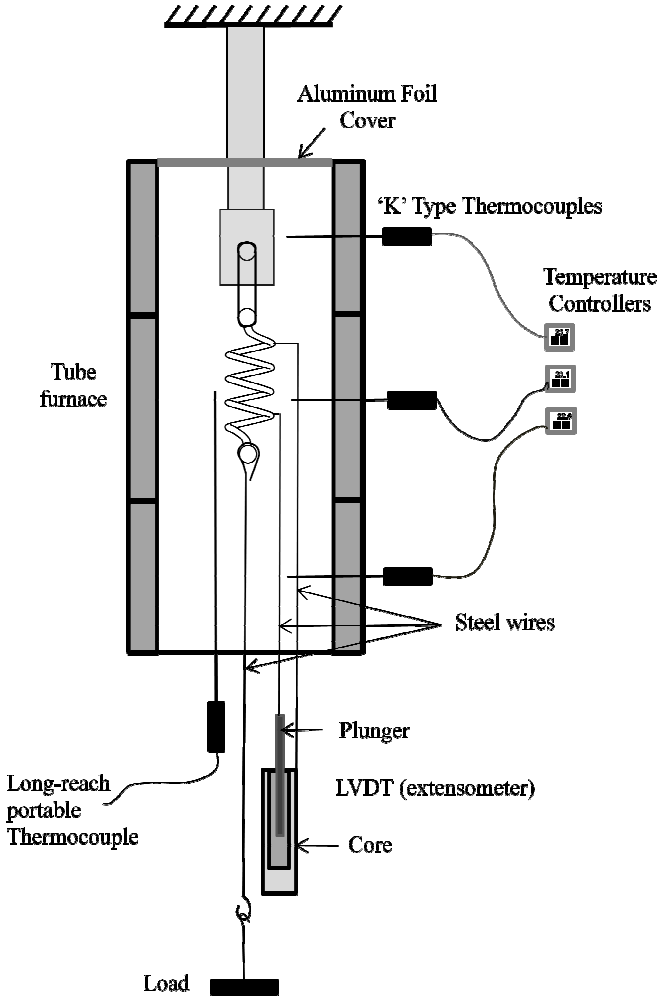

Figure 4.2. Schematic representaion of the creep apparatus

The sample is manually loaded and unloaded using a weight attached to a hook. Manual loading and unloading allows instantaneous response, which is especially needed for the recovery part of the test. The weight added by the two steel wires attached to the bottom of the sample and the plunger is 15 g and is therefore negligible compared to the

1.0-kg applied load. The top opening of the tube furnace is covered using aluminum foil to prevent excessive convection.

4.2 Furnace

The vertical tube furnace, 35 cm in length and 10 cm inside diameter, is reinforced with suitable material over the thickness that can act as insulator as well as handle temperatures up to 1500^{o}C. The furnace, shown in Figure 4.3, is divided into three independently controlled zones, each equipped with a thermocouple/controller system to maintain the inside temperature constant in time and space. Each individual zone has a hole through the thickness to accommodate a thermocouple.

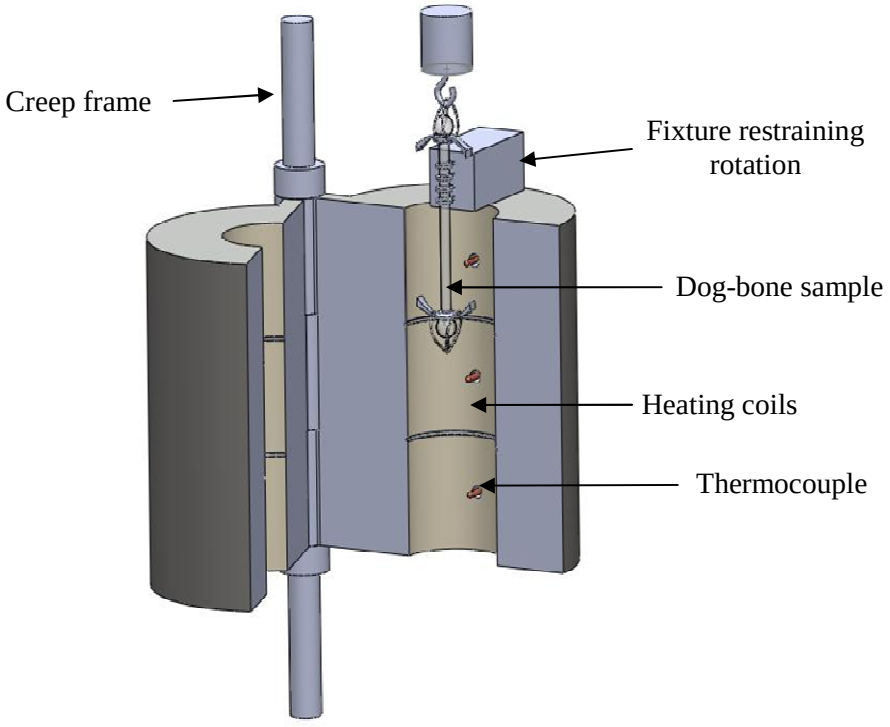

Figure 4.3. 3D-CAD model of a three zone tube furnace

A long range K-type thermocouple was used to develop a three-dimensional mapping of the temperature profile in axial and radial directions. Temperature is found uniform in the third zone of the furnace for a length of approximately 5 cm. Variation of temperature over this length is approximately ±3ºC.

Radial readings were measured over the diameter of the furnace for 1 cm increments in elevation and plotted as shown in Figure 4.4. From the figure it is evident that uniform temperature is present in the third zone of the furnace over a length of 5 cm approximately.

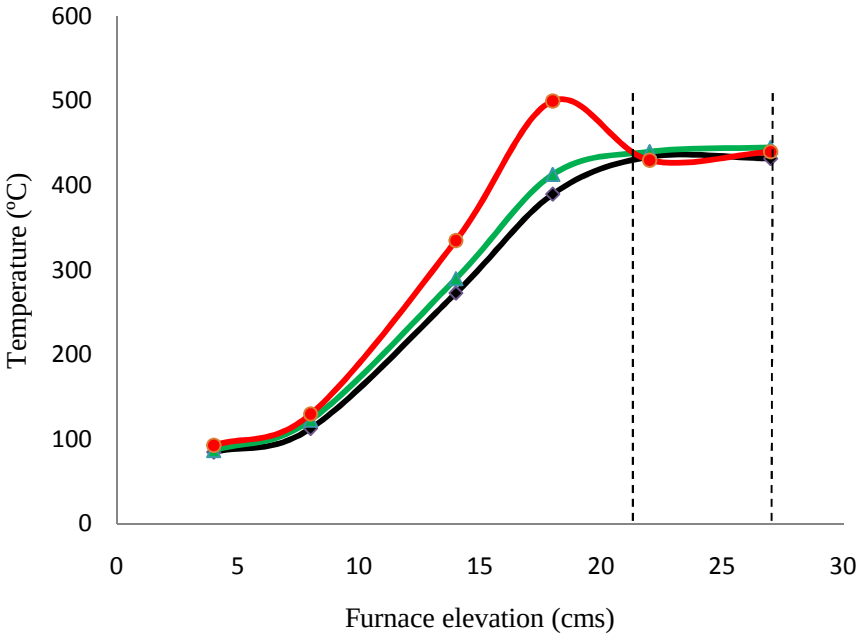

Figure 4.4. Temperature profiles in the axial direction for three radial positions: center axis (black), between center axis and furnace wall (green), near furnace wall (red)

From Figure 4.4, it can be inferred that there is an overlapping length of approximately 4 cm where temperature is uniform both axially and radially. This is the region where the sample is placed.

4.2 Extensometer

The extensometer is a linear variable displacement transducer (LVDT) used to measure the longitudinal displacement of spring and dog-bone samples. The LVDT is a frictionless induction device that measures the voltage difference due to downward and upward movement of the plunger inside the fixed core. Before assembling the LVDT with the experimental apparatus, it was calibrated using a calibrator with micron level accuracy. The measured sensitivity of the LVDT is 2.5 μm.

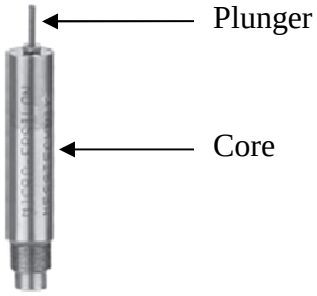

Figure 4.5. Linear variable displacement transducer

The linearity limit of the LVDT is only ±1 mm, i.e. 2 mm of linear region. However, during the creep-recovery experiments on spring sample, the ability to measure an extension of at least 4.5 mm is needed depending upon the dimensions of the sample. Therefore the LVDT was mapped in the non-linear region, as shown in Figure 4.6, and curve fitted to make use of the full 4.5-mm range of displacement. The curve-fit of the mapping is given by Equation (4.1):

$$y = 2.05e^{-06}x^6 + 1.87e^{-05}x^5 - 1.66e^{-03}x^4 + 2.46e^{-02}x^3 - 1.7e^{-01}x^2 + 9.56e^{-01}x - 6.09e^{-01} \quad (4.1)$$

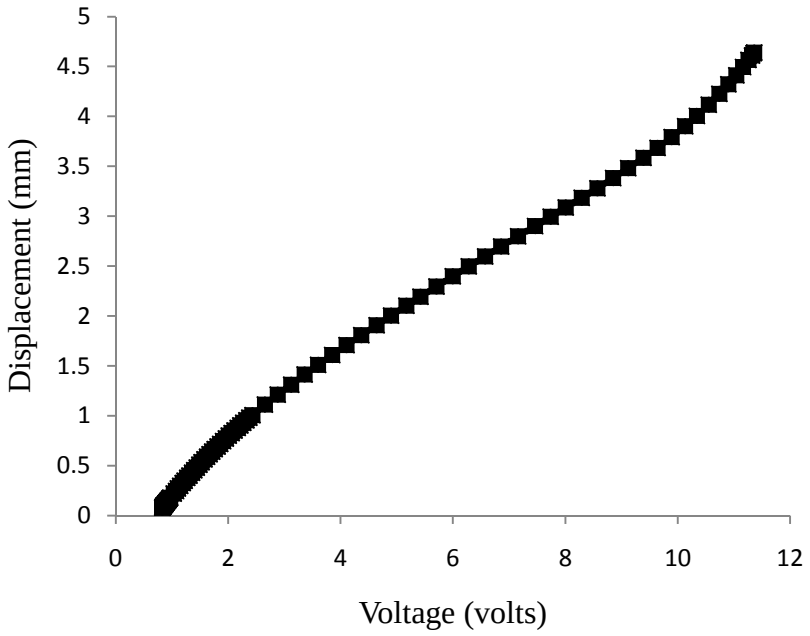

Figure 4.6. LVDT mapping

4.3 Reading through multi-meter and data acquisition card

Displacement of the plunger inside the core of a LVDT results in a change in voltage which was initially measured using a multimeter connected to a PC interface. The multimeter software installed on the PC allowed recording the voltage as a function time in a file with real time plotting capability as shown in Figure 4.7.

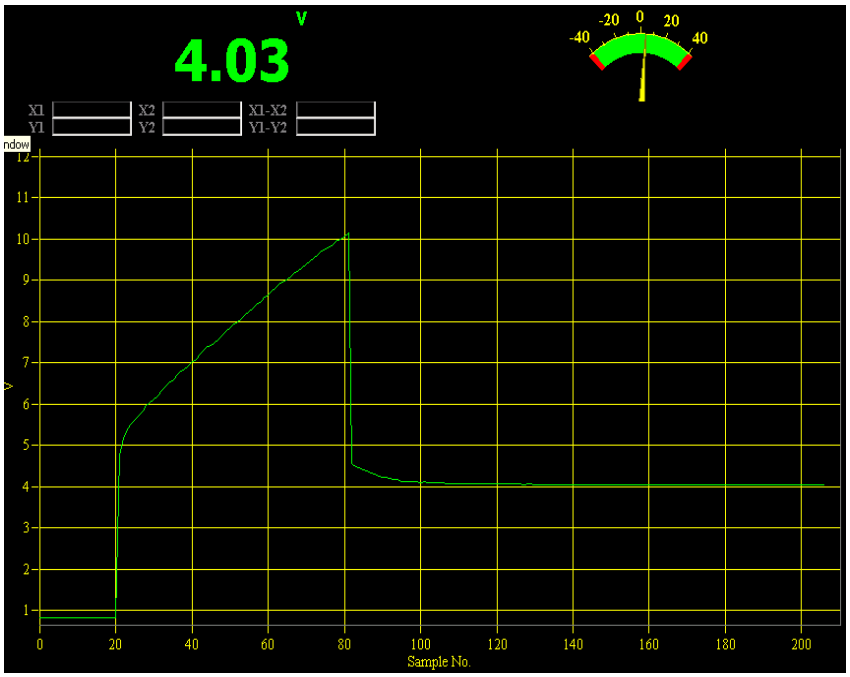

Figure 4.7. A sample multimeter reading

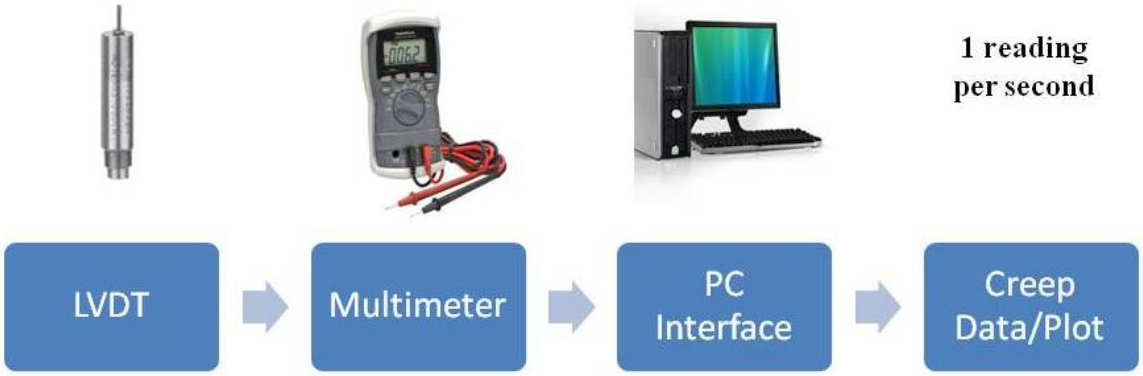

Figure 4.8. Operation chart using multimeter

The only limitation of this setup is the sampling period. Minimum sampling period provided by the software was limited to one second. But in order to differentiate between the instantaneous and the delayed portions of the creep-recovery curve it is necessary to have a sampling period equal to or less than one tenth of a second. Therefore

multimeter was replaced with a data acquisition system with a sampling rate of more than 10 readings per second. The software is incorporated with a feature of reducing noise through integration factor which can be input by the user. The wires can be grounded through the slot provided on board of the data acquisition card.

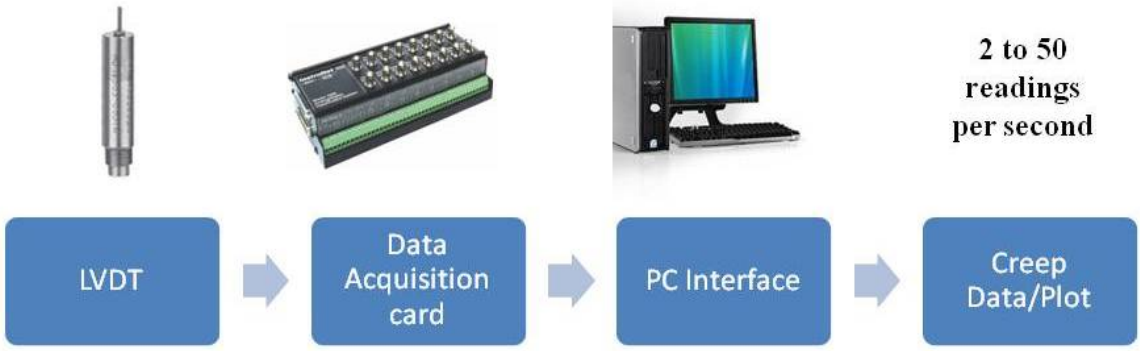

Figure 4.9. Operation chart using data acquisition card

4.4 Temperature controllers

Three temperature controllers as shown in Figure. 4.10 were employed to control the temperatures of the three individual zones of the furnace. They mainly consist of the display unit showing the current and target temperatures. Overshoot and undershoot range for the temperatures can also be input into the unit.

Figure 4.10 Temperature controller

Three K-type thermocouples projecting into each zone of the furnace through a small hole located in the middle of each zone are connected to the three temperature controllers. Three resistance temperatures detectors (RTD's) were initially used in place of the thermocouples for their higher sensitivity. However, albeit rated for the temperature of interest, they failed under the high temperature after a few experiments.

4.5 Gripping and orientation

Care should be taken while gripping the glass samples due to their property of fragileness. Grips are made of steel wires of almost negligible weight. These steel wires have the ability to withstand large loads at room and high temperatures. Hooks, wing nuts and screws are employed in the gripping process.

Spring sample

Spring sample is gripped on both sides using steel wires. It is fixed at the top position and bottom position is hooked to a long, thin steel rod projecting out of furnace with a provision of loading/ unloading. Extensometer is connected in between the points of interest on the sample as shown in Figure 4.11. Extensometer projections are connected to LVDT for displacement measurement.

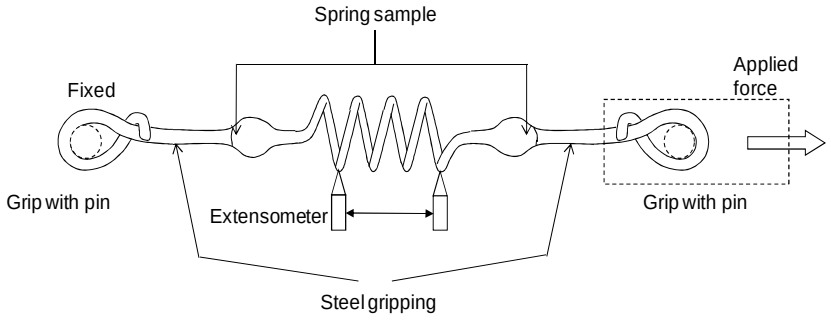

Figure 4.11 Gripping helical spring sample

Dog-bone sample

The main difficulty with dog-bone samples is to attach the extensometer wires to the glass rod. In the first attempts, the wires were fixed by wrapping them around the rod at a location reinforced with a piece of melted glass as shown in Figure 4.12. Even after careful annealing, weak spots were formed on the surface of the glass rod leading to breakage under loading. Alternatively, the extensometer wires were glued to the glass at room temperature using a small amount of glue. When placed in the furnace, the burned glue created enough friction to prevent sliding of the wires.

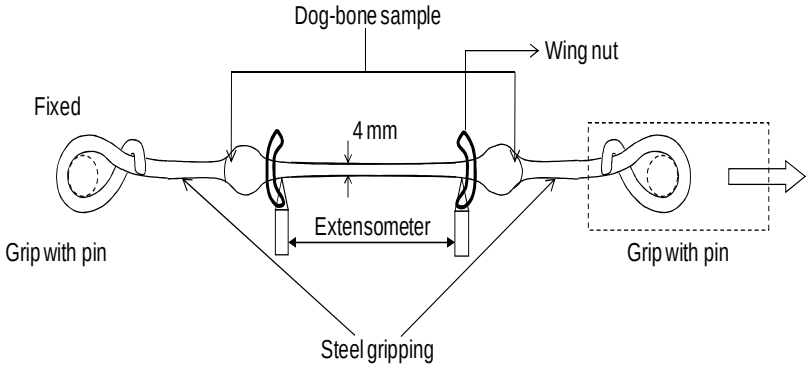

Figure 4.12 Gripping dog-bone sample

CHAPTER 5

PURE SHEAR EXPERIMENTS

5.1 Experimental Procedure

Shear creep-recovery experiments were performed on several helical spring samples at several temperatures in the transition region under several loads corresponding to stress levels between 3 and 12 MPa. In this thesis, we report the results of two temperatures, i.e., 563^{o}C and 588^{o}C, under a load of 8.89 N (i.e., 2.0 lbs), which corresponds to an average stress of 3.87 MPa through the coil's cross-section. The furnace is then heated to the temperature of interest and maintained long enough to reach a stabilized temperature. The creep test is then conducted as schematically described in Figure 5.1.

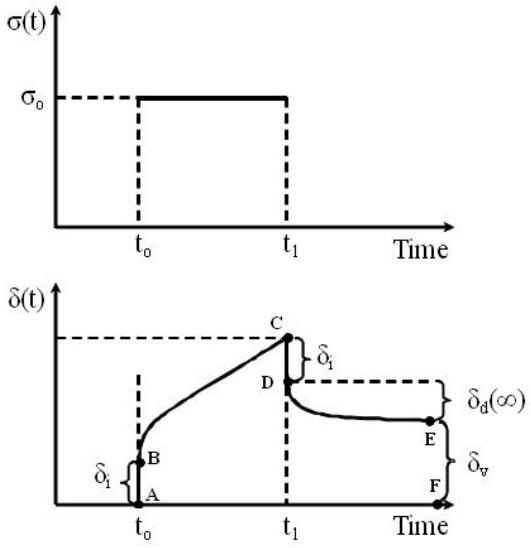

Figure 5.1. Creep-recovery curve

A 0.91-kg mass is instantaneously attached to the spring at time t_o yielding a stress σ_o, constant in time. The time-dependent displacement is then recorded. The stress is maintained until the displacement curve reaches a steady state. It is then instantaneously unloaded resulting into the instantaneous recovery followed by the time-dependent delayed recovery. In short the behavior of the creep curve can be described by the following four important features.

(1) The instantaneous response, δ_i, is the instantaneous elongation of the glass sample due to instantaneous application of stress and the instantaneous recovery due to instantaneous unloading. δ_i is shown in Figure 4 as segments AB and CD, which are equal in magnitude.

(2) The time-dependent loaded response (segment BC) is observed as long as the constant stress is applied.

(3) The delayed recovery, δ_d, (segment DE) corresponds to the time-dependent recovery.

(4) The Viscous part, δ_v, (segment EF)

The displacement measurement is recorded until the recovery curve becomes parallel to the time axis, i.e., changes in displacement are negligible or smaller than the resolution of the LVDT. The exact location of point D, which makes the transition between the instantaneous and the delayed parts, is determined by using the elongation from the same test of the sample at room temperature.

Figure 5.2 shows the creep-recovery curves of the glass spring sample with time at two different temperatures namely 563^{o}C and 587^{o}C with an average shear stress of 3.89 MPa.

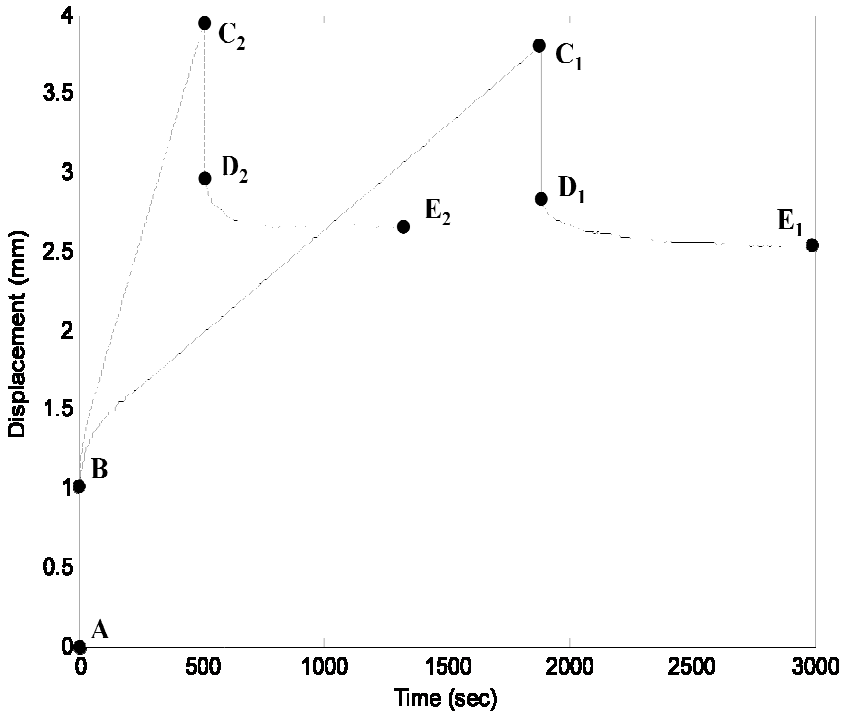

Figure 5.2. Displacement-time curves for 563^{o}C (solid) and 587^{o}C (dash) for borosilicate glass

5.2 Numerical treatment

Average strain calculation

Total shear stress at a given point (x,y) of the cross-section is the vector sum of the two stresses namely torsional stress and transversal stress.

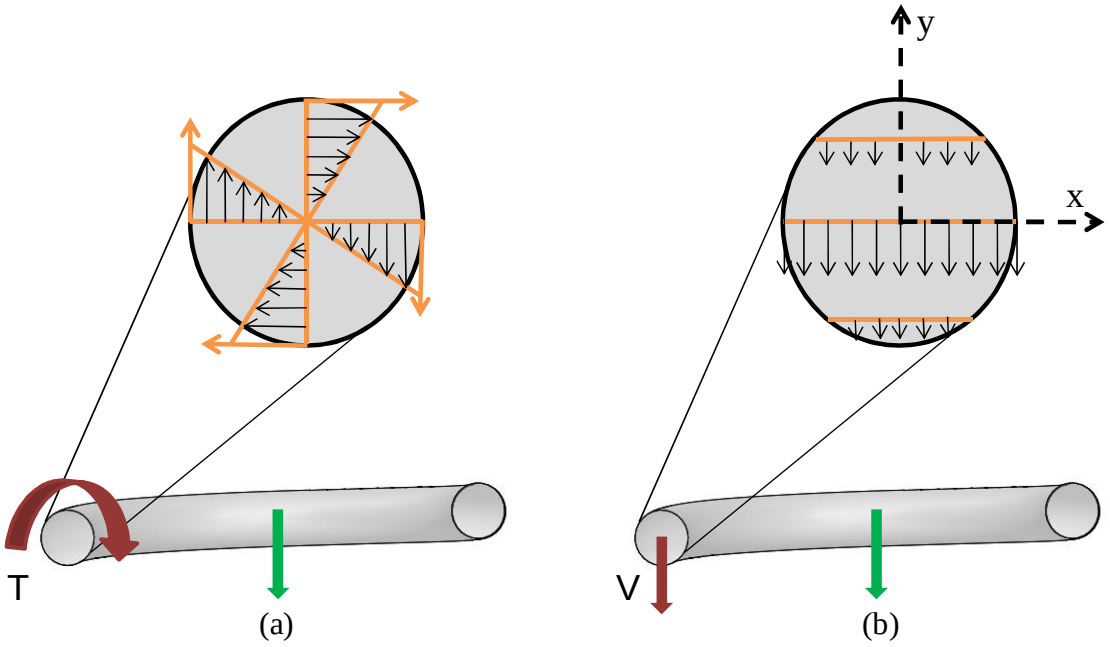

Figure 5.3 Stress distributions inside spring coil (a) torsional stress (b) transversal stress

Torsional stress inside the spring coil cross section is given by:

$$\tau_T = \frac{T\rho}{J} \tag{5.1}$$

where T is the torque, ρ is the radius and J is the polar moment of inertia.

Transversal stress inside the spring coil cross section is given by:

$$\tau_V(x,y) = \frac{VQ}{It} \tag{5.2}$$

where V is the transversal force, Q is the , I is the moment of inertia and t is the thickness of the cross section y.

The total average shear stress is the surface-averaged shear stress over the cross-section. Appendix [B] provides the MATLAB program developed to calculate the surface-averaged shear stress.

Displacement to shear strain conversion

The time dependent axial displacement of the spring is converted into time dependent shear-strain using the following relationship:

$$\gamma(t) = \left[\frac{8kD}{\pi d^3} + \frac{4k}{\pi d^2} \right] \delta(t) \tag{5.3}$$

where $\delta(t)$ and $\gamma(t)$ are the displacement (i.e., longitudinal elongation of the spring) and the maximum shear strain inside the coil, respectively, D and d are the pitch diameter and coil diameter of the spring sample, N is the number of coils between the attachments of the extensometers, and *k* is the geometric constant. Knowing the applied load F, the shear modulus G and the instantaneous elongation δ_i, the geometric constant *k* can be calculated using Eq. (5.4) given by Timoshenko and Young (1968).

$$F = kG\delta_i \tag{5.4}$$

The instantaneous elastic mechanical properties, namely, Young's modulus E and shear modulus G, of Borosilicate glass at the two tested temperatures are available in the literature, namely, Young's modulus: 64.25 GPa and 65 GPa and shear modulus: 25.9 GPa and 26.04 GPa at 563^{o}C and 587^{o}C, respectively [13]. Note that Duffrène et al. [7] neglected the variation of the mechanical properties of soda Lime Silicate glass in the transition region.

5.3 Viscosity calculation and temperature extraction

One of the issues related to the experimental procedure is the accurate measurement of the sample temperature. Even though we used several thermocouples around the sample, we extracted the temperature from published viscosity data. The

process consists of calculating the viscosity from the loading part of the strain-time curve (segment BC) of Figure 5.1 and makes use the published viscosity data of Borosilicate glass to extract the actual temperature of the sample.

The viscosity at the two test temperatures can be obtained by calculating the slope of the strain-time curve using the following equation [17]:

$$\eta = \frac{S_{12}}{2\theta} \tag{5.5}$$

where θ is the slope of the loaded part of the curve after reaching steady state, S_{12} is the shear stress applied on the spring sample and η is the viscosity at a given temperature. In this thesis, we use the shear stress averaged over the cross-section of the coil for S_{12} to account for the non-uniform stress distribution, which includes the torsional and transverse shear stress components whose formulas are available in any solid mechanics textbook.

We gathered the viscosity data of Borosilicate glass from two independent references [6, 12] and curve fitted the data as shown in Figure 7. Using Eq. (5.5), the viscosity at the two temperatures of interest are $10^{11.82}$ Pa.s and $10^{12.45}$ Pa.s. Figure 7 is then used to backtrack the corresponding temperatures, namely 563^{o}C and 588^{o}C, corresponding to the two viscosities.

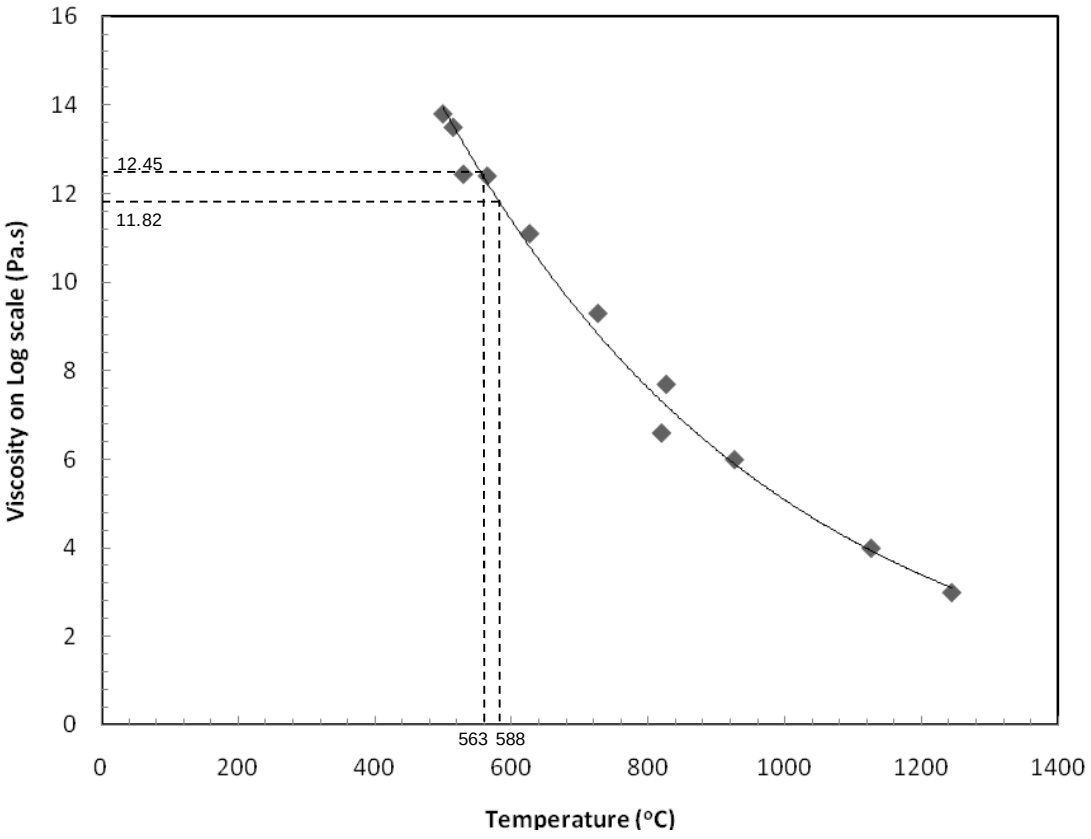

Figure 5.4. Temperature-dependent viscosity from two different references [6, 12]

5.4 Viscoelastic moments and constants

The previously mentioned viscoelastic moments and constants are needed in the next sections to determine the retardation and relaxation parameters. By calculating the viscosity at the test temperature, the relaxation viscoelastic moment $<\tau_1>$ can be determined using the so-called Maxwell relationship, which relates the viscosity and the shear modulus [7]:

$$<\tau_1> = \frac{\eta}{G} \tag{2.23}$$

The shear relaxation viscoelastic constant, H_t^2, is the ratio of total recovery to instantaneous recovery and is defined by [7, 10]:

$$H_t^{\,2} = \frac{<\tau_1^2>}{<\tau_1>^2} = \frac{\gamma_i + \gamma_d(\infty)}{\gamma_i} = 1 + \frac{\gamma_d(\infty)}{\gamma_i} \tag{2.22}$$

where $\gamma_d(\infty)$ is the total delayed strain recovery and γ_i is the instantaneous strain recovery. Both are calculated using Eqn. (6) knowing $\gamma_d(\infty)$ and γ_i, respectively.

The retardation curve, $\Phi(t)$, is obtained by normalizing the delayed strain recovery, $\gamma_d(t)$, with the total delayed strain from the strain-time curve as follows [7]:

$$\Phi(t) = \frac{\gamma_d(t)}{\gamma_d(\infty)} \tag{5.6}$$

The values of the viscoelastic moments and constants are calculated for the two temperatures of interest using Eqs. (2.22-2.24) and are given in Table 5.1.

	$<\tau_1>$	$<\lambda_1>$	$<\lambda_1^2>$	H_t^2	H_p^2	H_d^2
563°C	110.95	210.48	44997.95	1.19	1.016	3.335
588°C	26.01	62	4167.14	1.21	1.084	2.044

Table 5.1. Shear retardation/relaxation moments and constants

5.5 Determination of retardation parameters by curve fitting

Curve fitting is then carried out on the retardation function plotted on a semi-log scale using a Prony series as shown in Eqn. (5.9) with m_1 terms. In this research, we use $m_1 = 5$, which is sufficient to accurately describe the viscoelastic behavior of Borosilicate glass.

$$\Phi_1(t) = \sum_{j=1}^{m_1} \nu_{1j} \exp\left(\frac{-t}{\lambda_{1j}}\right) \tag{5.9}$$

The least-square error between the Prony series and the retardation curve was minimized while satisfying the following three constraints imposed on the retardation weights and times.

Eqn. (5.10) corresponds to the experimental retardation function with a mean time of 1 second as shown

$$\sum_{j=1}^{m1} \upsilon_{1j} = 1 \quad \text{and} \quad \upsilon_{1j} > 0 \tag{5.10}$$

Shear retardation moments are related to the parameters of shear retardation discrete spectrum as

$$< \lambda_1^{\alpha} >= \sum_{j=1}^{m1} \upsilon_{1j} \lambda_{1j}^{\alpha} \qquad , \alpha = 1, 2 \tag{5.11}$$

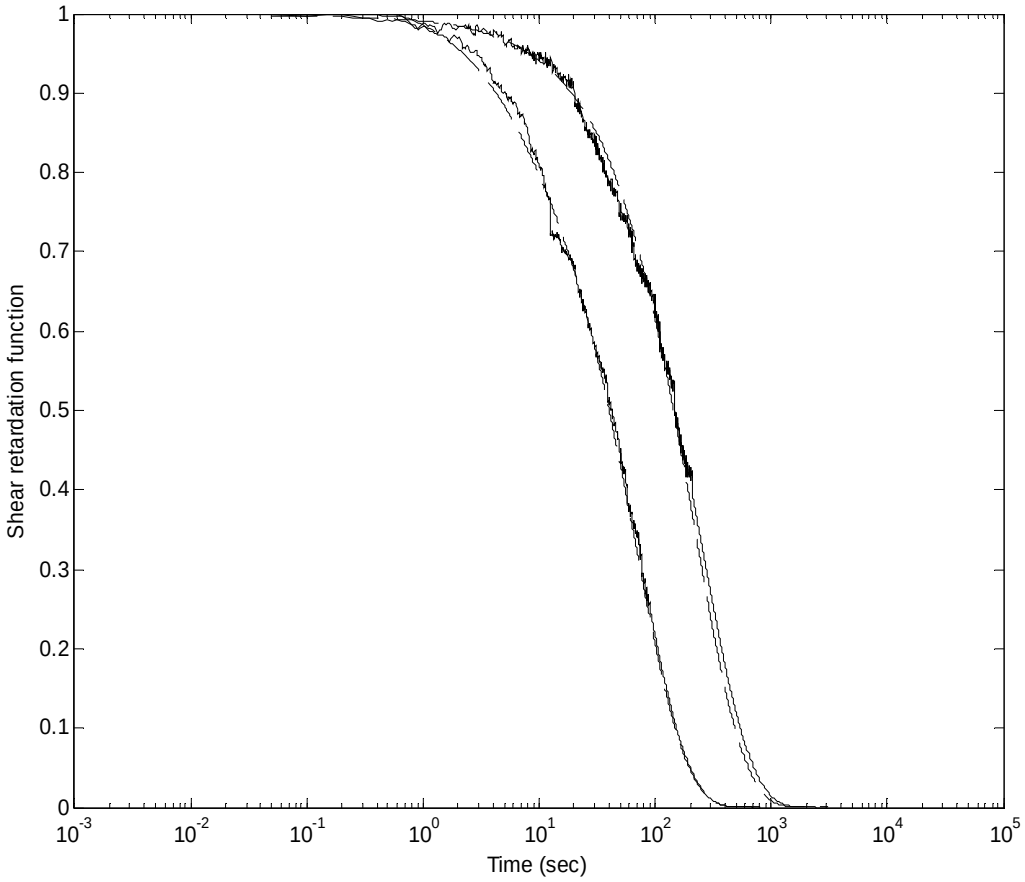

Figure 5.5. Retardation function vs. time with five-term Prony series, experimental (solid), fitted curve (dash) at 588^{o}C (left) and 563^{o}C (right)

563^{o}C		588^{o}C	
υ_{1j}	λ_{1j}	υ_{1j}	λ_{1j}
1.0E-06	1.5223E-07	1.00E-10	6.6033E-06
1.0E-04	1.0955E-04	1.00E-08	6.8031E-05
8.0E-04	0.8775	1.00E-07	1.1E-03
1.3121E-02	5.9777	0.0909725	5.1764
0. 9838	213.865	0.909027	67.68672

Table 5.2. Shear retardation parameters at two different temperatures

Retardation functions were successfully curve fit using a 5 term Prony series of a Generalized Maxwell model as shown in Figure 5.5 at two different temperatures. The retardation parameters are presented in Table 5.2

5.6 Retardation to Relaxation conversion

Once shear retardation parameters (retardation times and weights) are determined, they are transformed into relaxation parameters using the procedure in the literature by Gy *et al* [20]. (m+1) relaxation times are obtained by solving an (m+1) order equation as shown below

$$-p^2\Phi_1(p)\left(\frac{<\tau_1^2>}{<\tau_1>^2}-1\right)+p\left(\frac{<\tau_1^2>}{<\tau_1>^2}\right)+\left(\frac{1}{<\tau_1>}\right)=0 \qquad (5.11)$$

where Φ_1(p) is given by

$$\Phi_1(p)=\sum_{k=1}^{m1}\frac{\lambda_{1k}}{1+\lambda_{1k}p}\nu_{1k} \qquad (5.12)$$

This model takes into account the first shear relaxation viscoelastic constant and the viscoelastic parameter $<\tau_1>$. Eqn. (5.11) is solved for variable, p. Relaxation times are obtained by calculating the negative reciprocals of obtained, p, values.

Relaxation weights are determined from retardation and relaxation times. They are obtained by solving a system of linear equations, Eqn. (5.13), for the variable, p.

$$\psi_1\left(\frac{-1}{\lambda_{1k}}\right)=0 \qquad k = 1 \text{ to } m_1 \qquad (5.13)$$

where ψ(p) is given by,

$$\psi_1(p) = \sum_{k=1}^{m1} \frac{\tau_{1k}}{1+\tau_{1k}\,p} w_{1k} \tag{5.14}$$

Eqn. (5.13) consists of a system of 'm' linear equations. An additional equation is to be added to the system of linear equations to obtain (m+1) relaxation weights. This is given by

$$\psi_1(0) = <\tau_1> \tag{5.15}$$

563°C		588°C	
w_{1j}	τ_{1j}	w_{1j}	τ_{1j}
1.8973E-07	1.5225E-07	4.575E-7	6.6033E-06
1.8983E-06	1.0953E-04	2.1E-09	6.6803E-05
1.9568E-04	0.8773	2.09-08	1.0999E-03
3.0631E-03	5.9612	2.968E-02	5.05426
0.9703	97.446	0.91895	23.9288
0.0260	253.38	0.05136	75.352

Table 5.3. Shear relaxation parameters at two different temperatures

Table 5.3 presents the shear relaxation parameters obtained by applying the conversion process described above.

CHAPTER 6

SENSITIVITY ANALYSIS OF VARIOUS PROCESS VARIABLES ON RELAXATION PARAMETERS

6.1 Process variables at a glance

Sensitivity analysis of the process variable on relaxation parameters was carried out by altering process variables by 2%, 5% and 10%. Each process parameter is altered and its effect on relaxation weights and times is analyzed keeping retardation parameters constant since they completely depend on glass behavior. The effect of the process parameters on retardation weights and times is cancelled during the normalization process. Important process parameters include spring diameter, D, coil diameter, d, shear modulus, G, average shear stress, $\sigma_{average}$, and slope of the steady-state part of the loading curve, θ, which are directly or indirectly involved in retardation to relaxation conversion process. Two main conclusions that can be drawn from the sensitivity analysis:

1. Error in a process variable incorporates a linear error into relaxation weights and the last two relaxation times. There is negligible effect on four relaxation times.
2. Coil diameter, d, is the most significant process variable leading to approximately a three- to four-fold increase in error in relaxation weights and the last two times.

Section 5.6 describes the conversion of retardation parameters to relaxation parameters. From Eqn. (5.11) it can be inferred that $<\tau_1>$ is the variable responsible for variations in relaxation parameters and not the relaxation viscoelastic constant, since it is calculated from the glass behavior and not the process parameters. In this study the effect of process variables on relaxation moment $<\tau_1>$ is studied. Error in process variables leads to change

in $<\tau_1>$, which affects the relaxation times and since relaxation times are involved in calculation of relaxation weights as shown in Eqn. (5.5), they are indirectly affected. In all the cases shown below, relaxation times τ_5 and τ_6 are most active while others overlap with no deviation.

6.2 Spring diameter, D

Spring diameter and viscosity are indirectly related. Spring diameter is used in calculation of average shear stress as shown in Eqn. (5.1-5.2). From Eqn. (5.5) it is evident that the average shear stress is one of the main parameters that are responsible in viscosity calculation and it is related to $<\tau_1>$ using Eqn. (2.23). In brief spring diameter is directly proportional to relaxation viscoelastic moment $<\tau_1>$.

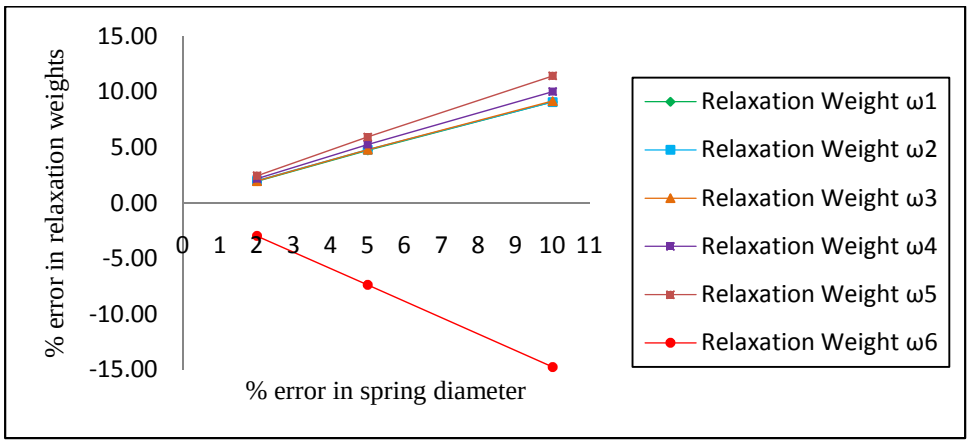

Figure 6.1. Sensitivity analysis of spring diameter on relaxation weights

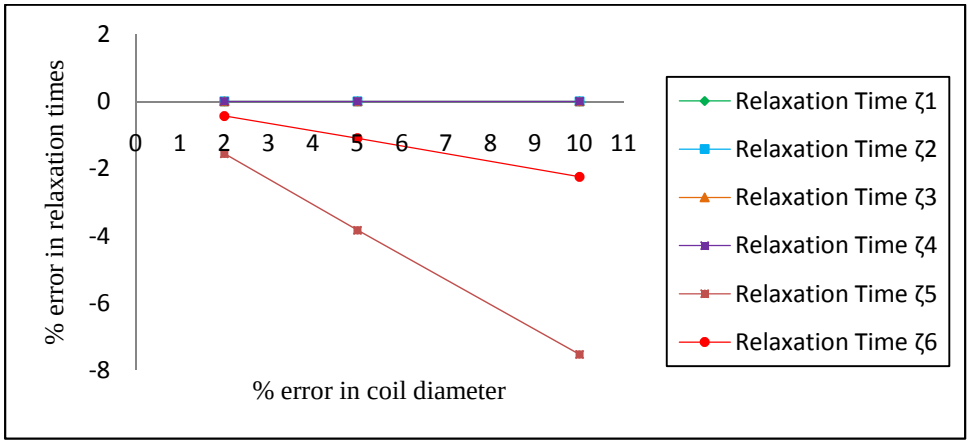

Figure 6.2. Sensitivity analysis of spring diameter on relaxation times

6.3 Coil diameter, d

Coil diameter is related to viscosity through average shear stress. Coil diameter is used in calculation of average shear stress as shown in Eqn. (5.1-5.2). From Eqn. (5.5) it is evident that average shear stress is one of the main parameters that are responsible in viscosity calculation and viscosity is related to $<\tau_1>$ using Eqn. (2.23). In brief coil diameter is inversely proportional to relaxation viscoelastic moment $<\tau_1>$.

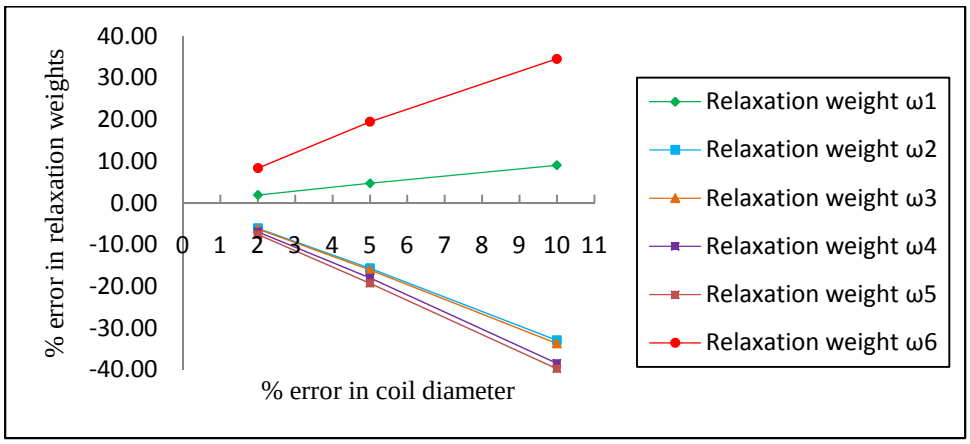

Figure 6.3. Sensitivity analysis of coil diameter on relaxation weights

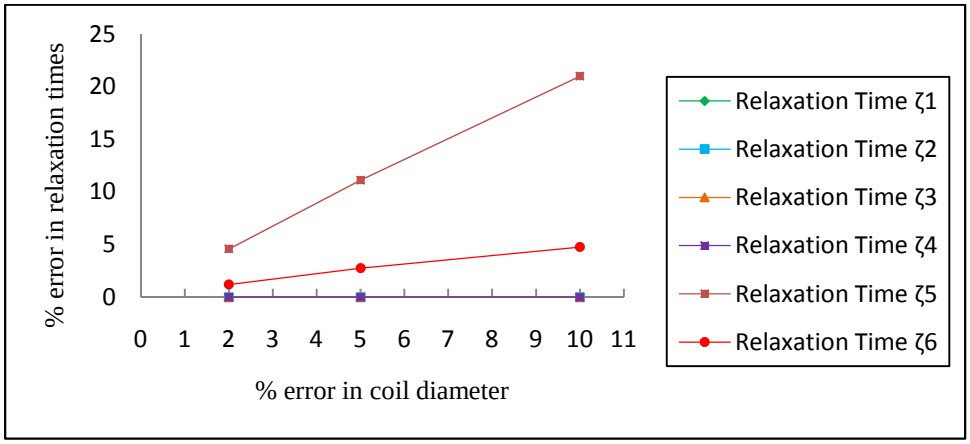

Figure 6.4. Sensitivity analysis of coil diameter on relaxation times

6.4 Shear modulus, G

From Eqn. (5.5), shear modulus is inversely proportional to <τ1> since

(1) <τ1> is directly involved in calculation of relaxation times and

(2) Relaxation times are involved in calculation of relaxation weights.

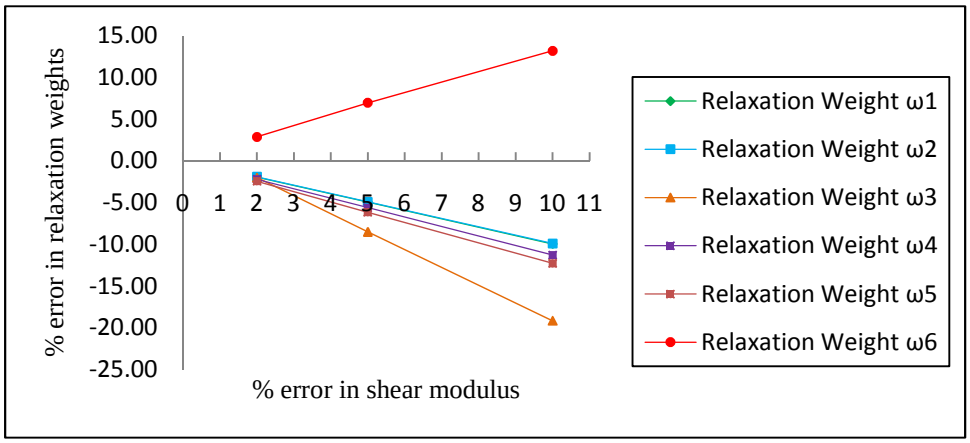

Figure 6.5. Sensitivity analysis of shear modulus on relaxation weights

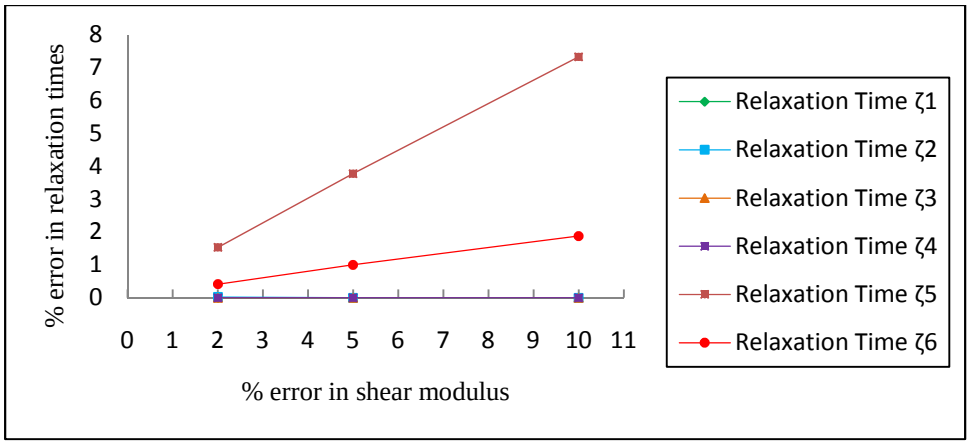

Figure 6.6. Sensitivity analysis of shear modulus on relaxation times

6.5 Load, L

From Eqn. (5.5) it is evident that average shear stress, σ_{avg}, is one of the main parameters that is responsible in viscosity calculation and it is related to $<\tau_1>$ using Eqn. (2.23). In brief applied load is directly proportional to relaxation viscoelastic moment $<\tau_1>$.

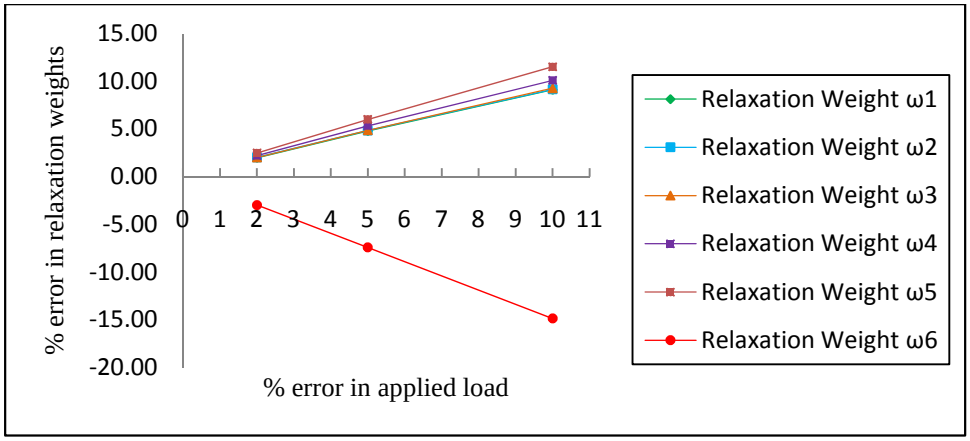

Figure 6.7. Sensitivity analysis of load on relaxation weights

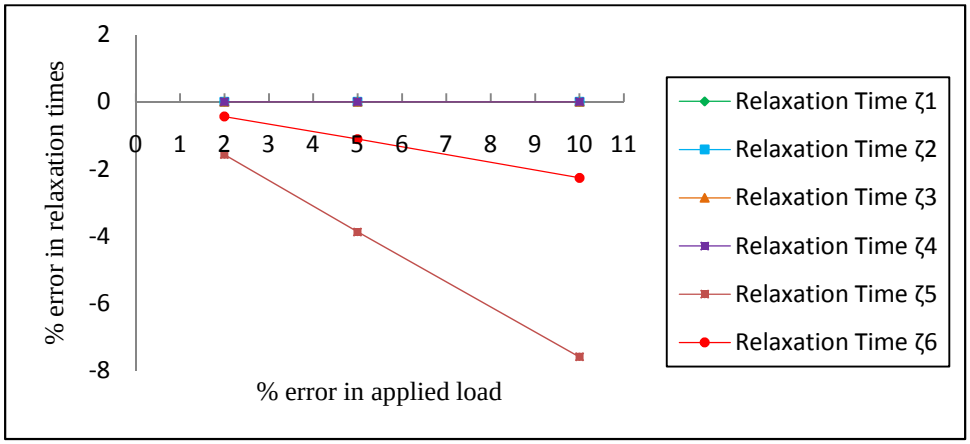

Figure 6.8. Sensitivity analysis of load on relaxation times

6.6 Slope, θ

Slope of the shear strain vs. time curve, θ, and average shear stress, σ_{avg}, are the two parameters used in viscosity calculation. Slope of the shear strain vs. time curve is inversely proportional viscosity and viscosity is directly proportional to <τ1>. In brief, slope of the shear strain vs. time curve is inversely proportional to <τ1>.

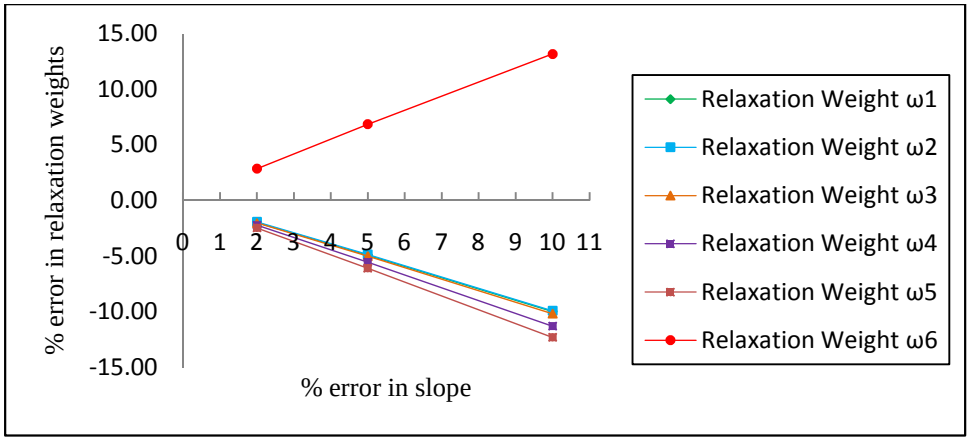

Figure 6.9. Sensitivity analysis of viscosity on relaxation weights

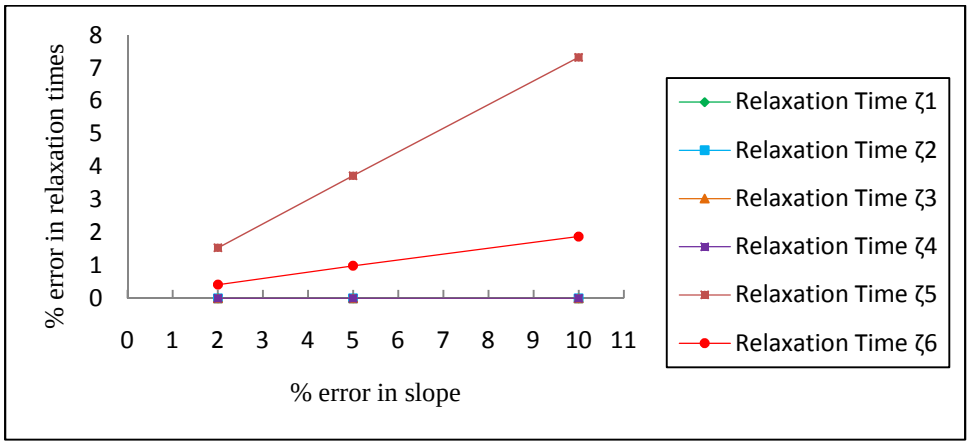

Figure 6.10. Sensitivity analysis of viscosity on relaxation times

CHAPTER 7

EXTRACTION OF HYDROSTATIC PARAMETERS

7.1 Introduction

All data pertaining to Shear is available in Chapter 5. The required data from shear experiments include retardation parameters, relaxation/retardation moments, viscoelastic constants and mechanical properties. Uni-axial creep recovery experiments were attempted on dog-bone samples at various temperatures and stress levels. However, the extension of the sample—of the order of 10 μm—could not be measured with the current setup because of overshadowing deformation due to rotation of the sample at loading and unloading. Nevertheless, this chapter presents the general procedure, the experimental issues, and the numerical treatment associated with extracting the hydrostatic parameters using a hypothetical curve.

Loads of higher magnitudes are required to deform the dog-bone samples to an appreciable amount. Care should be taken such that the applied stress does not exceed the upper limit of 12 MPa for glass to exhibit linear behavior. Initial dimensions of the sample are measured and placed inside the furnace where temperature gradient is negligible. The sample is soaked allowing glass to stabilize. The displacement-time curve is converted into a strain-time curve using Eqn. (7.1) below:

$$\varepsilon(t) = \frac{\Delta L}{L} \tag{7.1}$$

Strain is defined as the ratio of change in length to the original length. Analogous to shear creep-recovery experiments, numerical treatment of raw data involves isolation

of the delayed part from recovery curve knowing the instantaneous elongation through tension tests conducted at room temperature. The isolated delayed curve is shifted to the origin and then normalized resulting into a time-dependent uni-axial retardation function $\Phi_u(t)$ given by Eqn. (7.2).

$$\Phi_u(t) = \frac{\varepsilon(t)}{\varepsilon(\infty)} \tag{7.2}$$

where $\varepsilon(\infty)$ is the value of delayed recovery i.e. the value of maximum strain after shifting the isolated delayed curve to the origin and $\varepsilon(t)$ is time dependent recovery i.e. value of strain at a given time, t on the shifted curve. The retardation function $\Phi_u(t)$ ranges between 1 and 0 i.e. $\Phi_u(0) = 1$ and $\Phi_u(\infty) = 0$.

The bulk modulus K_g is calculated from Eqn. (7.3) knowing the moduli of elasticity and rigidity, E and G, at a given temperature.

$$\frac{1}{E} = \frac{1}{9K_g} + \frac{1}{3G} \tag{7.3}$$

Since it is difficult to conduct experiments to measure the bulk equilibrium modulus K_e, it is calculated from Eqn. (7.4) [21].

$$\frac{1}{E}\left(1 + \frac{\sigma_u^{\,2}}{<\tau_u^{\,2}>}\right) = \frac{1}{3G}\left(1 + \frac{\sigma_1^{\,2}}{<\tau_1^{\,2}>}\right) + \frac{1}{9K_e} \tag{7.4}$$

where E and G are moduli of elasticity, σ_1 and σ_u are the shear stress and uni-axial stress respectively, $<\tau_1>$ and $<\tau_u>$ are the relaxation moments in shear and uni-axial respectively.

7.2 Hydrostatic viscoelastic moments and constants

As mentioned earlier, viscoelastic constants and moments are dimensionless parameters with some physical meaning discussed in Chapter 2. The theory on viscoelastic moments, constants and their conversions applied in this research is based on a series of published papers by L. Duffrène and R. Gy [7, 10, 20, 21]. Uni-axial relaxation moment $<\tau_u>$ is calculated knowing the viscosity, η, and Young's modulus, E, using Eqn. (7.5).

$$\eta = G < \tau_1 >= \frac{E < \tau_u >}{3} \tag{7.5}$$

The uni-axial relaxation viscoelastic constant is calculated from the resultant strain-time curve and is defined as the ratio of total recovery to instantaneous recovery as shown in Eqn. (7.6).

$$\frac{< \tau_u^{\,2} >}{< \tau_u >^2} = \frac{\varepsilon_d(\infty) + \varepsilon_i}{\varepsilon_i} \tag{7.6}$$

Hydrostatic retardation moments are associated with area under the retardation function versus time curve. They are incorporated into the curve fitting process as constraints on retardation weights and times. To calculate the hydrostatic retardation moments, $<\lambda_2^{\alpha}>$, α = 1,2, as shown in Eqn. (7.8), values of uni-axial retardation moments , $<\lambda_u^{\alpha}>$, α = 1,2, calculated using Eqn. (7.7) and shear retardation moments , $<\lambda_1^{\alpha}>$, α = 1,2,calculated using Eqn. (2.23-2.24) are needed.

$$< \lambda_u^{\,\alpha} >= \frac{1}{\Gamma(\alpha)} \int_0^{\infty} t^{(\alpha-1)} \Phi_u(t) \tag{7.7}$$

$$\frac{1}{E}\left(\frac{<\tau_u^{\,2}>}{<\tau_u>^2}-1\right)<\lambda_u^{\,\alpha}>=\frac{1}{3G}\left(\frac{<\tau_1^{\,2}>}{<\tau_1>^2}-1\right)<\lambda_1^{\,\alpha}>+\left(\frac{1}{9K_e}-\frac{1}{9K_g}\right)<\lambda_2^{\,\alpha}> \qquad (7.8)$$

Hydrostatic retardation constants can be determined from the uni-axial retardation constant and the shear retardation constant as shown in Eqn. (7.9).

$$\frac{<\lambda_2^{\,2}>}{<\lambda_2>^2}=\frac{3\left(\frac{<\tau_u^{\,2}>}{<\tau_u>^2}-1\right)}{(1-2\nu)\left(\frac{K_g}{K_e}-1\right)}\frac{<\lambda_u^{\,2}>}{<\lambda_u>^2}\left(\frac{<\lambda_u>}{<\lambda_2>}\right)^2-\frac{2(1+\nu)\left(\frac{<\tau_1^{\,2}>}{<\tau_1>^2}-1\right)}{(1-2\nu)\left(\frac{K_g}{K_e}-1\right)}\frac{<\lambda_1^{\,2}>}{<\lambda_1>^2}\left(\frac{<\lambda_1>}{<\lambda_2>}\right)^2$$

(7.9)

Hydrostatic relaxation constant is then derived from retardation constant knowing the bulk modulus, K_g, and equilibrium modulus, K_e.

$$\left(\frac{<\lambda_2^{\,2}>}{<\lambda_2>^2}-1\right)=\frac{K_g}{K_e}\left(\frac{<\tau_2^{\,2}>}{<\tau_2>^2}-1\right) \qquad (7.10)$$

7.3 Curve fit for hydrostatic retardation parameters

As mentioned earlier uni-axial retardation function encompasses both shear and hydrostatic retardation functions. Hydrostatic parameters can be separated from the uni-axial retardation function using Eqn. (7.11) knowing the shear retardation parameters. Subscripts 1 and 2 refer to the shear and hydrostatic parameters, respectively.

$$\Phi_u(t)=A\left[\sum_{k=1}^{m_1}\nu_{1,k}\exp^{\frac{-t}{\lambda_{1,k}}}\right]+B\left[\sum_{k=1}^{m_2}\nu_{2,k}\exp^{\frac{-t}{\lambda_{2,k}}}\right] \qquad (7.11)$$

where constants A and B are given by

$$A = \frac{2(1+\nu)}{3} \frac{\left(\frac{<\tau_1^{\,2}>}{<\tau_1>^2} - 1 \right)}{\left(\frac{<\tau_u^{\,2}>}{<\tau_u>^2} - 1 \right)} \tag{7.12}$$

$$B = \frac{(1-2\nu)}{3} \frac{\left(\frac{K_g}{K_e} - 1 \right)}{\left(\frac{<\tau_u^{\,2}>}{<\tau_u>^2} - 1 \right)} \tag{7.13}$$

Shear retardation parameters are available from Chapter 5 Table 5.1. Apart from satisfying the main equation, the hydrostatic retardation parameters need to satisfy the constraining Eqn. (7.14) and Eqn.(7.15) for α equal to 1 and 2.

$$\sum_{j=1}^{m} \nu_{2,j} = 1 \tag{7.14}$$

$$\sum_{j=1}^{m} \nu_{2,j} \lambda_{2,j}{}^{\alpha} = <\lambda^{\alpha}> \tag{7.15}$$

where ν_{2j}, j=1,…m, is greater than zero.

7.4 Retardation to relaxation conversion

Retardation parameters are converted to relaxation parameters by solving a polynomial equation for relaxation times and a system of linear equations for relaxation weights. Theory and relevant equations utilized in this section are from a published paper by R. Gy *et al.* [20].

Eqn. (7.16) shows a polynomial equation that must be solved for hydrostatic relaxation times. It is a *n*-th degree polynomial equation in terms of *p*. The *n* relaxation times are negative reciprocals of the *n* roots obtained from solving this equation.

$$p(K_g - K_e)\left[\sum_{k=1}^{m}\lambda_{2,k}\nu_{2,k}\prod_{j\neq k}(1+\lambda_{2,j}p)\right] - K_g\prod_{k=1}^{m}(1+\lambda_{2,k}p) = 0 \qquad (7.16)$$

Relaxation weights are obtained by solving a system of *n* linear equations as shown in Eqn. (7.17) to obtain *n* hydrostatic relaxation weights.

$$\sum_{j=1}^{n}\frac{\tau_{2,j}}{\lambda_{2.k}+\tau_{2,j}}w_{2,j} = -\frac{K_e}{(K_e - K_g)} \qquad (7.17)$$

7.5 Application to hypothetical curve

Several uni-axial creep-recovery experiments were attempted on dog-bone glass samples to extract meaningful recovery data. However, as explained earlier, this turned out to be a great challenge since the extension of glass rod is of the order of a few microns as compared to a few millimeters in the case of spring samples.

As the elongation of a cylindrical glass rod was in an order of several microns, sufficient data couldn't be extracted by the employed L.V.D.T. In order to explain the process of extracting the hydrostatic parameters and to estimate the level of accuracy needed in the process of uni-axial testing, a hypothetical curve was developed. Figure 7.1 shows a hypothetical strain-time curve constructed based on estimations such as

1) Instantaneous elongation calculated theoretically
2) Time dependent elongation as per temperature calculated through viscosity
3) Delayed region calculated indirectly from Eqn. (7.12)

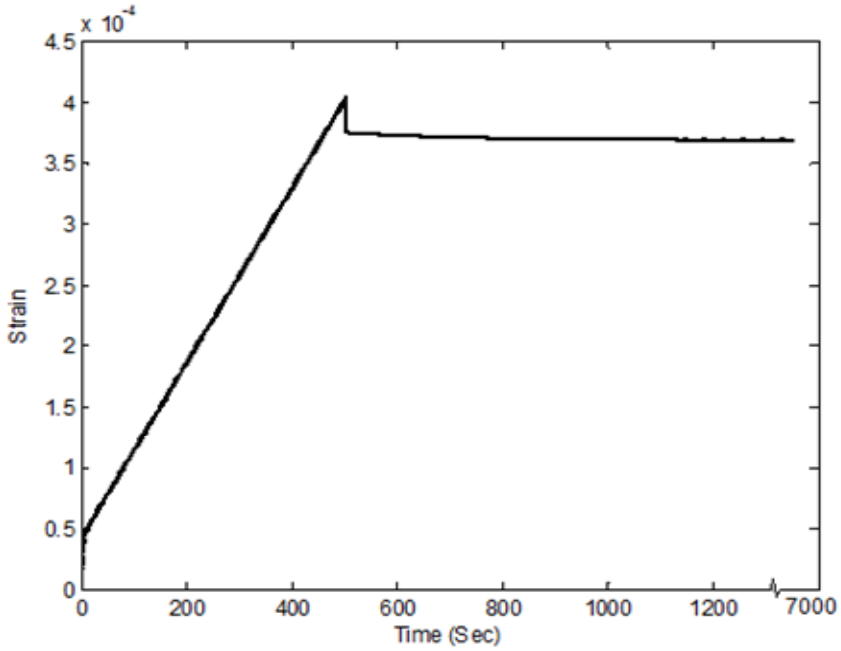

Figure 7.1 Hypothetical strain-time curve at 563^{o}C

The process of numerical treatment explained in Sections 7.1 and 7.2 was carried out on the hypothetical data. The uni-axial retardation function is curve fitted for hydrostatic retardation parameters knowing the shear retardation parameters as explained in Section 7.3. Figure 7.2 shows the experimental curve fitted using a 5 term Prony series of a Generalized Maxwell model. The uni-axial retardation function is fitted for hydrostatic parameters as shown in Eqn. (7.11).

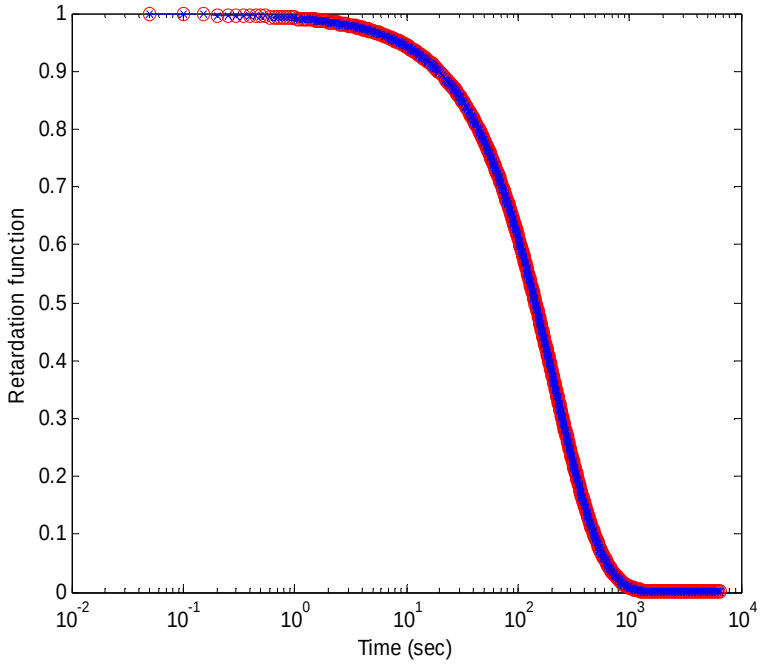

Figure 7.2 Retardation function vs. time with five term Prony series, hypotheticall (red),fitted curve (blue) at 563^{o}C

Hydrostatic retardation parameters are then converted to relaxation parameters using the relevant equations as explained in section 7.4. Table 7.1 shows the hydrostatic retardation and relaxation parameters for the hypothetical curve at 563^{o}C.

υ_{1j}	λ_{1j}	ω_{2j}	τ_{2j}
1.0E-08	1.00001E-08	2.00065E-08	1.0000999E-08
1.0E-06	9.99986E-08	2.00048E-06	9.99985E-08
1.0E-04	1.02131E-01	2.00009E-04	0.100203
0.4999478	199.999936	0.999799	100.0528
0.49995118	200	5.1108E-14	199.99996

Table 7.1 Hydrostatic retardation and relaxation parameters at 563^{o}C

Issues

One of the major issues that arise during uni-axial creep-recovery experiments is the overshadowing effect on elongation of sample by rotation during loading and

unloading since the sample couldn't be perfectly aligned with the vertical axis due to the attached extensometer assembly. Other issues include (1) failure of sample due to weak spots formed during flame working and (2) creep data being below LVDT's sensitivity value. Ideally it is required to increase load to maximum stress or increase the length of the sample to increase the sensitivity. It is not possible to increase the length of the sample since temperature uniformity zone inside the furnace is limited. Stress can be increased only up to a limit of 12 MPa, crossing which leads to non linear behavior of glass.

CHAPTER 8

CONCLUSION AND FUTURE WORK

8.1 Conclusion

The intent of this thesis is to provide the foundation and the initial ground work for further study on stress relaxation of optical glasses, which present challenging issues for conducting the required experiments. The research presented in this thesis includes the following main contributions:

(1) Investigated the experimental procedure for conducting creep-recovery experiments on glass, specifically optical low-T_g glasses, near the transition temperature. This investigation includes manufacturing of glass samples, experimental apparatus, temperature control and displacement sensing ability.

(2) Developed of a step-by-step procedure for extracting shear and hydrostatic stress-relaxation parameters from creep experimental data. The procedure is based on the theory of viscoelasticity of glass presented in a set of scattered publications.

(3) Highlighted limitations of current experimental setup for shear and uni-axial experiments in terms of temperature uniformity and displacement sensitivity.

8.2 Future work

Based on the experience gathered during this research project, the following recommendations for future work include:

(1) Acquire the experimental capability to measure sub-micron measurement of deformation to perform uni-axial creep-recovery experiments on dog-bone samples to

extract hydrostatic relaxation parameters. Alternatively, larger samples should be used, which brings issues related to temperature uniformity along the sample.

(2) Creep (i.e., force-controlled) and stress relaxation (i.e., displacement-control) experiments are complementary. This research focused on creep since a known force can be easily applied using gravity. However, stress relaxation may have to be conducted as opposed to creep in the case of uni-axial experiment because of the sub-micron sensitivity needed to measure the creep-recovery curve. Alternatively, stress relaxation tests would require control of the final deformation which would be of the order of several micrometers. A load cell with sensitivity of the order of 0.1 lbf may provide sufficient information.

(3) Use Finite Element Analysis to validate the stress-relaxation parameters determined experimentally by modeling the experimental sample behavior in shear and uni-axial.

(4) Through the sensitivity analysis carried out in Chapter 6 it is evident that there is a linear dependence of shear modulus on shear relaxation parameters. Thus, the assumption of mechanical properties to be constant over the transition temperature range should be revisited.

(5) Manufacturing spring samples out of low T_g optical glasses is challenging therefore consider:

- Manufacturing in controlled environment inside a tube furnace at low temperature,
- Consider a pure shear experiment through torsion

APPENDICES

Appendix A

Temperature dependent mechanical properties of Pyrex® glass

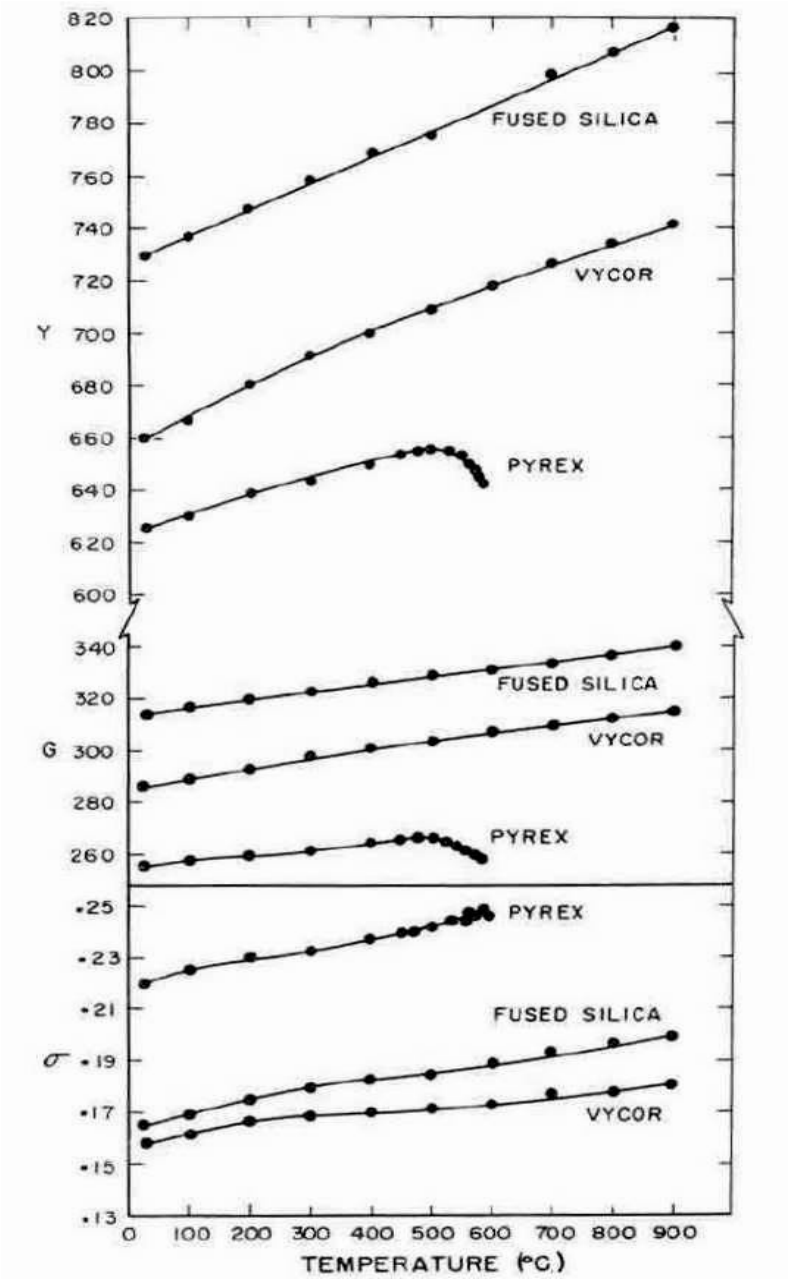

Figure A-1: Temperature dependent mechanical properties of Pyrex® [13]

Appendix B

MATLAB program for determining shear retardation parameters

Master program 'Viscoelastic_characterization.m'

```
clc
clear all
close all
format long
%--------------------------------------------------------------------------
% Loading raw creep data i.e. volatage vs. time data
load Ch4_Vin+.TXT;
%--------------------------------------------------------------------------
Ch4 = Ch4_Vin_;
deltaT= 0.025;
%--------------------------------------------------------------------------
extract1 = [];
i = length(Ch4);
x = max(Ch4);
while Ch4(i) < x
    extract1 = [extract1;Ch4(i)];
        i = i-1;
end
extract2 = [];
for i=1:length(extract1)
    extract2(i,1) = extract1(length(extract1)-i+1);
    time_vector(i,1) = deltaT*i;
end
figure
plot(extract2,'.')
hold on
plot(extract2,'r-')
%--------------------------------------------------------------------------
% Voltage to displacement conversion based on curvefit equation
Lim = size(extract2,1);
for (i=1:Lim)
     displacement(i,1) = 0.205322e-5*((3.95*extract2(i,1))^6)+...
         0.186968e-4*((3.95*extract2(i,1))^5)-...
         0.165999e-2*((3.95*extract2(i,1))^4)+...
         0.24609133e-1*((3.95*extract2(i,1))^3)-...
         0.170434241*((3.95*extract2(i,1))^2)+...
         0.956249924*((3.95*extract2(i,1))^1) - 0.609482469;
end
figure
plot(time_vector,displacement,'.')
hold on
plot(time_vector,displacement,'r-')
%Enter the Instantaneous Elongation(mm)from Tension test (room temperature)
instantaneous = input('\n Enter the Instantaneous Elongation(mm):');
```

```
% Noise removal
integrate = 1;
Nint = 11; % must be odd number 3, 5, 7, 9
disp_integrated = displacement;
if integrate
 for i=(Nint-1)/2+1:length(displacement)-(Nint-1)/2
   disp_integrated(i) = sum(displacement(i-(Nint-1)/2:i+(Nint-1)/2))/Nint;
 end
    displacement = disp_integrated;
end
extract3 = [];
time_vector3 = [];
for i=2:length(displacement)
    if displacement(1)-displacement(i) >= instantaneous
        extract3 = [extract3;displacement(i)];
        time_vector3 = [time_vector3;time_vector(i)];
    end
end
time_vector3_shifted = time_vector3-min(time_vector3);
figure
plot(time_vector3_shifted,extract3,'.')
hold on
plot(time_vector3_shifted,extract3,'r-')

%--------------------------------------------------------------------------
% User input
fprintf('Welcome To Creep-Recovery Program\n');
E = input('\n Input Youngs Modulus of the Material(MPa) : ');
G = input('\n Input Bulk Modulus of the Material(MPa) : ');
D = input('\n Input Helical Spring diameter(mm) : ');
d = input('\n Input coil diameter of the spring(mm) : ');
N = input('\n Input number of turns in the spring sample : ');
M = input('\n Input the load on helical spring sample(Lbs) : ');

%Acceleration due to gravity
g = 9.81;
%Pound to Kg conversion
CF = 0.45359237;
F = M*g*CF;
pi = 3.14157;
% Spring shape factor 'k' from Hookes law
k = F/(G*instantaneous);

%--------------------------------------------------------------------------
% Axial displacement to Shear strain conversion
Strain_factor = (((8*k*D)/((pi)*d^3)) + ((4*k)/((pi)*d^2)))
strains = Strain_factor*extract3;
figure
plot(time_vector3_shifted,strains,'.')
hold on
plot(time_vector3_shifted,strains,'r-')
```

```
% Shifting strains to origin
strains_at_zero = strains-min(strains);
plot(time_vector3_shifted,strains_at_zero,'k.')
plot(time_vector3_shifted,strains_at_zero,'m-')

%-------------------------------------------------------------------------
% Normalization process
normalized_strains = strains_at_zero/max(strains_at_zero);
figure
plot(time_vector3_shifted,normalized_strains,'k.')
hold on
plot(time_vector3_shifted,normalized_strains,'m-')

%-------------------------------------------------------------------------
% First and second retardation moment calculation
total_area = 0;
for i=1:length(normalized_strains)-1
   total_area = total_area+(normalized_strains(i)+...
      normalized_strains(i+1))/2*deltaT;
end
total_area

second_moment = 0;
for i=1:length(normalized_strains)-1
   second_moment = second_moment+(time_vector3_shifted(i)+...
      time_vector3_shifted(i+1))/2*(normalized_strains(i)+...
      normalized_strains(i+1))/2*deltaT;
end
second_moment

figure
semilogx(time_vector3_shifted,normalized_strains,'k.')
hold on
semilogx(time_vector3_shifted,normalized_strains,'m-')
m = length(time_vector3_shifted);

%-------------------------------------------------------------------------
%Writes the data to a file
fid = fopen('retardationcurve.m','w');
fprintf(fid,'%s\n','retardation = [');
for i=1:length(time_vector3_shifted)
   fprintf(fid,'%s\n',num2str([time_vector3_shifted(i,:),...
      normalized_strains(i,1)]));
end
fprintf(fid,'%s','];');
fclose(fid);

%-------------------------------------------------------------------------
%Invokes the curve fitting program main.m
main
```

MATLAB program for curve fitting, ‘main.m’

```
% fmincon is used to extract stress relaxation constants from a retardation curve
clc
clear all
close all
warning off
format long;
options = optimset();
params = [44997.95, 210.48 ,1];
%-------------------------------------------------------------------------
X0 = [       1e-09,   1.00e-07,...
             1e-07,   1.00e-06,...
             1e-06,   1.00e-05,...
             1e-02,          5,...
               0.9,         50];
LB = [      1e-10,        1e-6,…
             1e-07,       1e-3,…
             1e-08,       1e-5,…
             1e-02,          1,…
             1e-01,       1e-5];
UB = [          1,         100,…
                1,         100,…
                1,         100,…
                1,         100,
                1,         100];
%-------------------------------------------------------------------------

 [sol,fmin] = fmincon('objfun',X0,[],[],[],[],LB,UB,'confun_ineq',options,params)
retardationcurve

semilogx(retardation(:,1),retardation(:,2),'ro')
xlabel('Time (sec)')
ylabel('Retardation function')
hold on
semilogx(retardation(:,1),retard_approx(sol,retardation(:,1)),'x--')

figure
semilogx(retardation(:,1),retardation(:,2),'k')
xlabel('Time (sec)')
ylabel('Retardation function')
hold on
semilogx(retardation(:,1),retard_approx(sol,retardation(:,1)),'k--')

fid = fopen('curve1.m','w');
for i=1:length(retardation)
   fprintf(fid,'%s\n',num2str([retardation(i,:),retard_approx(sol,retardation(i,1))]));
end
fclose(fid);
```

Subprogram ‘objfun.m’

```
function y = objfun(x,params)

retardationcurve;

y = 0;
for i=1:size(retardation,1)
   y = y+(retardation(i,2)-retard_approx(x,retardation(i,1)))^2;
end
```

Subprogram ‘retard_approx.m’

```
% Prony series with 5 terms

function r = retard_approx(x,t)

r = x(1)*exp(-t/x(2)) + x(3)*exp(-t/x(4)) + x(5)*exp(-t/x(6)) + x(7)*exp(-t/x(8)) + x(9)*exp(-t/x(10));
```

Subprogram ‘confun_ineq.m’

```
function [C,Ceq] = confun(x,params)

C = [abs(x(1)+x(3)+x(5)+x(7)+x(9))-params(3);...
      abs(x(1)*x(2)+x(3)*x(4)+x(5)*x(6)+x(7)*x(8)+x(9)*x(10))-params(2);...
      abs(x(1)*x(2)^2+x(3)*x(4)^2+x(5)*x(6)^2+x(7)*x(8)^2+x(9)*x(10)^2)-params(1);];
Ceq = [];
```

Subprogram ‘retardationcurve.m’

```
% Refer master program
Retardation = [
time       normalized strains
];
```

Program to calculate average shear stress inside the spring coil

```
clc
clear all
close all
D = 26.365
d = 4.77
G = 25400
M = 2
F = (0.45359237)*(9.80665)*(M);
slope = 8.008700E-07
nrhos = 11
nthetas = 36
rho = 0
delta_rho = d/2/(nrhos-1)
delta_theta = 360/nthetas
numerator = 0;
denominator = 0;
figure
plot(0,0,'.')
hold on
store = [];
for i=1:nrhos
   theta = 0;
   for j=1:nthetas
      sigma_tors = F*D/2*rho/(pi*d^4/32);
      sigma_tors_X = sigma_tors*sin(theta*pi/180);
      sigma_tors_Y = sigma_tors*cos(theta*pi/180);
      sigma_tran = 6*F/d^4*(d^2/4-(rho*sin(theta*pi/180))^2);
      sigma_tran_X = 0;
      sigma_tran_Y = -sigma_tran;
      sigma_total_X = sigma_tors_X+sigma_tran_X;
      sigma_total_Y = sigma_tors_Y+sigma_tran_Y;
      sigma_total = sqrt(sigma_total_X^2+sigma_total_Y^2);
      store = [store; sigma_tors, sigma_tran, sigma_total];
      if sigma_total > 3
         plot(rho*cos(theta*pi/180),rho*sin(theta*pi/180),'g.')
      else
         plot(rho*cos(theta*pi/180),rho*sin(theta*pi/180),'r.')
      end
      dA = rho*delta_theta*pi/180*delta_rho;
      numerator = numerator+sigma_total*dA;
      denominator = denominator+dA;
      theta = theta+delta_theta;
   end
   rho = rho+delta_rho
end
% numerator
% denominator
surface_average = numerator/denominator
axis equal
min(store)
```

max(store)

viscosity = log10(((surface_average)/(2*slope))*10^6)
Temperature = -log(viscosity/38.283)/0.002
tau_moment = ((surface_average)/(2*slope))/G

Appendix C

MAPLE program for shear retardation-to-relaxation conversion

$$Retardation := \begin{bmatrix} 0.0000000001 & 0.000006603300047 \\ 0.00000001 & 0.000068031121889 \\ 0.0000001 & 0.0011 \\ 0.0909725193 & 5.1764429224 \\ 0.909027370505670 & 67.68 \end{bmatrix}$$

$$x := \left(\frac{Retardation(1,1)}{p + \left(\frac{1}{Retardation(1,2)}\right)}\right) + \left(\frac{Retardation(2,1)}{p + \left(\frac{1}{Retardation(2,2)}\right)}\right) + \left(\frac{Retardation(3,1)}{p + \left(\frac{1}{Retardation(3,2)}\right)}\right) + \left(\frac{Retardation(4,1)}{p + \left(\frac{1}{Retardation(4,2)}\right)}\right) + \left(\frac{Retardation(5,1)}{p + \left(\frac{1}{Retardation(5,2)}\right)}\right)$$

$$MainEquation := -0.21\,p^2\,x + 1.21\,p + \frac{1}{26.01};$$

$$Relaxationtime := solve(MainEquation = 0)$$

$$-0.01327214463, -0.04179115307, -0.1978528900, -909.0909282, -14699.15495, -1.51439430710^5$$

$$Relaxationtimes := \begin{bmatrix} \frac{-1}{-1.51439510^{5}} \\ \frac{-1}{-14699.15495} \\ \frac{-1}{-909.0909282} \\ \frac{-1}{-0.1978528803} \\ \frac{-1}{-0.04179115307} \\ \frac{-1}{-0.01327214463} \end{bmatrix}$$

```
for i from 1 to 5 do
    for j from 1 to 6 do
Ret := (i, j) → ( Relaxationtimes(j, 1) / (1 + ((Relaxationtimes(j, 1)) * (-1 / Retardation(i, 2)))) );
Retardationparam := Matrix(5, 6, Ret);
  od
od
```

```
solve({
        Relaxationtimes(1, 1) · w1 + Relaxationtimes(2, 1) · w2
    + Relaxationtimes(3, 1) · w3 + Relaxationtimes(4, 1) · w4
    + Relaxationtimes(5, 1) · w5 + Relaxationtimes(6, 1) · w6
    = 26.01,

                                        Retardationparam(1, 1)
    · w1 + Retardationparam(1, 2) · w2 + Retardationparam(1, 3)
    · w3 + Retardationparam(1, 4) · w4 + Retardationparam(1, 5)
    · w5 +  Retardationparam(1, 6) · w6 = 0,

                                        Retardationparam(2, 1)
    · w1 + Retardationparam(2, 2) · w2 + Retardationparam(2, 3)
    · w3 + Retardationparam(2, 4)· w4 + Retardationparam(2, 5)
    · w5 +  Retardationparam(2, 6) · w6 = 0,

                                        Retardationparam(3, 1)
    ·w1 + Retardationparam(3, 2)·w2 + Retardationparam(3, 3)·w3
    + Retardationparam(3, 4)·w4 + Retardationparam(3, 5)·w5
    +  Retardationparam(3, 6)·w6 = 0,

                                        Retardationparam(4, 1)
    ·w1 + Retardationparam(4, 2)·w2 + Retardationparam(4, 3)·w3
    + Retardationparam(4, 4)·w4 + Retardationparam(4, 5)·w5
    +  Retardationparam(4, 6)·w6 = 0,

                                        Retardationparam(5, 1)·w1
     + Retardationparam(5, 2)·w2 + Retardationparam(5, 3)·w3
    + Retardationparam(5, 4)·w4 + Retardationparam(5, 5)·w5
    +  Retardationparam(5, 6)·w6 = 0}, {w1, w2, w3, w4, w5, w5,
    w6})
```

$$\{w1 = 4.57500322910^{-7}, w2 = 2.10000621910^{-9}, w3 = 2.09010325310^{-8}, w4 = 0.0296805344, w5 = 0.9189419009, w6 = 0.05137749269\}$$

Appendix D

MATLAB program for determining hydrostatic retardation parameters

```
% fmincon is used to extract stress relaxation constants from a retardation curve
clc
clear all
close all
warning off
format long;
% pause(0.1)
options = optimset();
params = [3.999902102838096e+004, 1.999975502968964e+002,1];
X0 = [ 1e-8,   1e-8,  1e-6,    1e-7,   1e-8,   150,   1e-6,   150,   1e-4,  1e-1];
LB = [ 1e-8,   1e-8,  1e-6,    1e-7,   1e-8,   100,   1e-6,   150,   1e-4,  1e-1];
UB = [    1,    100,     1,     100,     1,   200,   0.998,    200,      1,  100];
[sol,fmin] = fmincon('objfun',X0,[],[],[],[],LB,UB,'confun_ineq',options,params)
retardationcurve
semilogx(retardation(:,1),retardation(:,2),'ro')
xlabel('Time (sec)')
ylabel('Retardation function')
hold on
semilogx(retardation(:,1),retard_approx(sol,retardation(:,1)),'x--')
figure
semilogx(retardation(:,1),retardation(:,2),'k')
xlabel('Time (sec)')
ylabel('Retardation function')
hold on
semilogx(retardation(:,1),retard_approx(sol,retardation(:,1)),'k--')
fid = fopen('Retardation_data.m','w');
for i=1:length(retardation)
   fprintf(fid,'%s\n',num2str([retardation(i,:),retard_approx(sol,retardation(i,1))]));
end
fclose(fid);
solution = sol';
for (m = 1:5)
    Parameter(m,1) = solution(2*m,1);
end
for (m = 1:5)
Parameter(m,2) = solution(2*m-1,1);
end
fid = fopen('Ret_param.m','w');
fprintf(fid,'%s\n','retardation_parameters = [');
for (j = 1:5)
fprintf(fid,'%s  %s\n',[Parameter(j,1),Parameter(j,2)]);
end
fprintf(fid,'%s','];');
fclose(fid);
```

Subprogram ‘objfun.m’

```
function y = objfun(x,params)

retardationcurve;

y = 0;
for i=1:size(retardation,1)
   y = y+(retardation(i,2)-retard_approx(x,retardation(i,1)))^2;
end
```

Subprogram ‘retard_approx.m’

```
% Prony series with 5 terms

function r = retard_approx(x,t)
r = 0.8*(    1.00E-06*exp(-t/1.5223E-07)...
          + 1.00E-04*exp(-t/1.0955E-04)...
          + 8.00E-04*exp(-t/0.8775)...
          + 1.3121E-02*exp(-t/5.9777)...
          + 0.9838*exp(-t/213.8655)        )+ ...
   0.20*(    x(1)*exp(-t/x(2))...
          + x(3)*exp(-t/x(4))...
          + x(5)*exp(-t/x(6))...
          + x(7)*exp(-t/x(8))...
          + x(9)*exp(-t/x(10))...
          );
```

Subprogram ‘confun_ineq.m’

```
function [C,Ceq] = confun(x,params)

C = [abs(x(1)+x(3)+x(5)+x(7)+x(9))-params(3);...
       abs(x(1)*x(2)+x(3)*x(4)+x(5)*x(6)+x(7)*x(8)+x(9)*x(10))-params(2);...
       abs(x(1)*x(2)^2+x(3)*x(4)^2+x(5)*x(6)^2+x(7)*x(8)^2+x(9)*x(10)^2)-params(1);];
Ceq = [];
```

Subprogram ‘retardationcurve.m’

```
% Refer master program
Retardation = [
time        normalized strains
];
```

Appendix E

MAPLE program for shear retardation-to-relaxation conversion

$$Hyrel := \begin{bmatrix} 0.00000001 & 0.000000010001 \\ 0.000001 & 0.0000000999986 \\ 0.0001 & 0.1002131704541 \\ 0.499947808130 & 5199.9999361142282 \\ 0.499951181869 & 5200.0000000000000 \end{bmatrix}$$

$$Result := simplify(p.(Kg - Ke) \cdot ((Hyrel(1,2) \cdot Hyrel(1,1)) \cdot ((1 + p \cdot Hyrel(2,2)) \cdot (1 + p \cdot Hyrel(3,2)) \cdot (1 + p \cdot Hyrel(4,2)) \cdot (1 + p \cdot Hyrel(5,2))) + (Hyrel(2,2) \cdot Hyrel(2,1)) \cdot ((1 + p \cdot Hyrel(1,2)) \cdot (1 + p \cdot Hyrel(3,2)) \cdot (1 + p \cdot Hyrel(4,2)) \cdot (1 + p \cdot Hyrel(5,2))) + (Hyrel(3,2) \cdot Hyrel(3,1)) \cdot ((1 + p \cdot Hyrel(1,2)) \cdot (1 + p \cdot Hyrel(2,2)) \cdot (1 + p \cdot Hyrel(4,2)) \cdot (1 + p \cdot Hyrel(5,2))) + (Hyrel(4,2) \cdot Hyrel(4,1)) \cdot ((1 + p \cdot Hyrel(1,2)) \cdot (1 + p \cdot Hyrel(2,2)) \cdot (1 + p \cdot Hyrel(3,2)) \cdot (1 + p \cdot Hyrel(5,2))) + (Hyrel(5,2) \cdot Hyrel(5,1)) \cdot ((1 + p \cdot Hyrel(1,2)) \cdot (1 + p \cdot Hyrel(2,2)) \cdot (1 + p \cdot Hyrel(3,2)) \cdot (1 + p \cdot Hyrel(4,2)))) - Kg \cdot ((1 + p \cdot Hyrel(1,2)) \cdot (1 + p \cdot Hyrel(2,2)) \cdot (1 + p \cdot Hyrel(3,2)) \cdot (1 + p \cdot Hyrel(4,2))))$$

$$solve(Result, p)$$

$$-0.005000000794, -0.009994716129, -9.979725817, -1.00001500010^{7}, -9.99900019510^{7}$$

$$Relatim := simplify\left(\begin{bmatrix} \frac{-1}{-9.99900019510^{7}} \\ \frac{-1}{-1.00001500010^{7}} \\ \frac{-1}{-9.979725817} \\ \frac{-1}{-0.009994716129} \\ \frac{-1}{-0.005000000794} \end{bmatrix}\right)$$

$$Term := -\frac{Ke}{(Ke - \mathrm{Kg})}$$

$$
\begin{aligned}
&solve\Bigg(\Bigg\{\frac{Relatim(1,1)}{Hyrel(1,2)-Relatim(1,1)}\cdot w1\\
&\quad+\frac{Relatim(2,1)}{Hyrel(1,2)-Relatim(2,1)}\cdot w2\\
&\quad+\frac{Relatim(3,1)}{Hyrel(1,2)-Relatim(3,1)}\cdot w3\\
&\quad+\frac{Relatim(4,1)}{Hyrel(1,2)-Relatim(4,1)}\cdot w4\\
&\quad+\frac{Relatim(5,1)}{Hyrel(1,2)-Relatim(5,1)}\cdot w5=Term,\\
&\quad\frac{Relatim(1,1)}{Hyrel(2,2)-Relatim(1,1)}\cdot w1\\
&\quad+\frac{Relatim(2,1)}{Hyrel(2,2)-Relatim(2,1)}\cdot w2\\
&\quad+\frac{Relatim(3,1)}{Hyrel(2,2)-Relatim(3,1)}\cdot w3\\
&\quad+\frac{Relatim(4,1)}{Hyrel(2,2)-Relatim(4,1)}\cdot w4\\
&\quad+\frac{Relatim(5,1)}{Hyrel(2,2)-Relatim(5,1)}\cdot w5=Term,\\
&\quad\frac{Relatim(1,1)}{Hyrel(3,2)-Relatim(1,1)}\cdot w1\\
&\quad+\frac{Relatim(2,1)}{Hyrel(3,2)-Relatim(2,1)}\cdot w2\\
&\quad+\frac{Relatim(3,1)}{Hyrel(3,2)-Relatim(3,1)}\cdot w3\\
&\quad+\frac{Relatim(4,1)}{Hyrel(3,2)-Relatim(4,1)}\cdot w4\\
&\quad+\frac{Relatim(5,1)}{Hyrel(3,2)-Relatim(5,1)}\cdot w5=Term,\\
&\quad\frac{Relatim(1,1)}{Hyrel(4,2)-Relatim(1,1)}\cdot w1\\
&\quad+\frac{Relatim(2,1)}{Hyrel(4,2)-Relatim(2,1)}\cdot w2\\
&\quad+\frac{Relatim(3,1)}{Hyrel(4,2)-Relatim(3,1)}\cdot w3\\
&\quad+\frac{Relatim(4,1)}{Hyrel(4,2)-Relatim(4,1)}\cdot w4\\
&\quad+\frac{Relatim(5,1)}{Hyrel(4,2)-Relatim(5,1)}\cdot w5=Term,\\
&\quad\frac{Relatim(1,1)}{Hyrel(5,2)-Relatim(1,1)}\cdot w1\\
&\quad+\frac{Relatim(2,1)}{Hyrel(5,2)-Relatim(2,1)}\cdot w2\\
&\quad+\frac{Relatim(3,1)}{Hyrel(5,2)-Relatim(3,1)}\cdot w3\\
&\quad+\frac{Relatim(4,1)}{Hyrel(5,2)-Relatim(4,1)}\cdot w4\\
&\quad+\frac{Relatim(5,1)}{Hyrel(5,2)-Relatim(5,1)}\cdot w5=Term\Bigg\},\{w1,w2,w3,w4,\\
&\quad w5,w5\}\Bigg);
\end{aligned}
$$

REFERENCES

[1] http://www.toshiba-machine.co.jp/english

[2] Jain A., A. Y. Yi, "Numerical Modeling of Viscoelastic Stress Relaxation during Glass Lens Molding Process," *J. Am. Ceram. Soc*., 88(2005), pp. 530-535.

[3] Mazurin, O.V, Streltsina, M.V., and Totesh, A.S., "The viscosity and transformation temperature of phase separated sodium borosilicate glasses," *Phys. and Chemisty of Glasses*, 10 (1969) 63-68.

[4] Uhlmann D.R. and Kreidl N.J., *Viscosity and phase transition, Vol 3: Viscosity and Relaxation*, Academic Press, Orlando, FL., 1986.

[5] Ananthasayanam B, *Computational molding of precision molding of aspheric glass optics*, Ph.D. Thesis, Clemson University, 2008.

[6] Rekhson S., "Viscosity and stress relaxation in commercial glasses in the glass transition region," *Journal of non-crystalline solids* 38 & 39 (1980), 457-462.

[7] Duffrène L., R.Gy, H. Burlet R. Piques, "Multiaxial linear viscoelastic behavior of a soda-lime-silica glass based on a generalized Maxwell model," *Journal of Non-Crystalline Solids*, Vol. 215, pp. 208-217, 1997.

[8] Steven N. Crichton and Simon M. Rekhson, "Measuring stress relaxation in a compression relaxometer," *Journal of Non-crystalline solids*, 142 (1992) pp. 133-147.

[9] Rekhson S., "Models of relaxation in glass," *Journal of Non-Crystalline Solids*, Vol. 95-96, pp. 131-148, 1987.

[10] Duffrène L., Gy R., "Viscoelastic constants of a Soda-Lime-Silica glass," *Journal of non-crystalline solids* Vol. 211, pp. 30-38, 1997.

[11] Rekhson S.M. "Linear and Non-Linear Viscoelasticity of Glass," *Journal of non-crystalline solids*, Vol 42, pp. 185 1980.

[12] Pascual M.J, Pascual L., Dran A., "Determination of the viscosity-temperature curve for glasses on the basis of fixed viscosity points determined by hot stage microscopy," *Physics and chemistry of Glasses*, Vol. 42 (2001), pp. 61-66

[13] Spinner S, "Elastic Moduli of Glasses at Elevated Temperatures by a Dynamic Method," *American ceramic society*, Vol. 39, pp. 113-118, 1955.

[14] Corning data sheet, www.matweb.com

[15] http://www.arlon-med.com/Measuring and Understanding Tg.pdf

[16] Malkin A.Y. and Isayev A.I., *Rheology - Concepts, Methods, & Applications*, ChemTec Publishing, ISBN: 978-1-895198-33-1.

[17] Scherer G. W., *Relaxation in Glass and Composites*, 4th Ed., Wiley-Interscience.

[18] Tchoegl N.W., *The phenomenological theory of linear viscoelastic behavior: An introduction*, Springer, Paris, 1989.

[19] Technical discussion with Dr. Fotheringham U., Adjunct professor, Clemson University.

[20] Gy R., Duffrène L., Labrot M., "New insights into viscoelasticity of glass," *Journal of non-crystalline solids*, Vol. 175, pp. 103-117, 1994.

[21] Gy R., "On the equilibrium isothermal compressibility of soda-lime silicate glass," *Journal of non-crystalline solids*, Vol. 128, pp. 101-108, 1991.